

ScholarWorks@GSU

The Geochemical Trends of Major and Select Trace Elements through a Soil Profile Near Mt. Daisen, Japan

Authors	Jackson, Cynthia
Citation	Jackson, Cynthia. The Geochemical Trends of Major and Select Trace Elements through a Soil Profile Near Mt. Daisen, Japan. Dec. 2015, Georgia State University. https://doi.org/10.57709/7559284 .
DOI	https://doi.org/10.57709/7559284
Download date	2026-04-11 01:49:24
Link to Item	https://hdl.handle.net/20.500.14694/6468

THE GEOCHEMICAL TRENDS OF MAJOR AND SELECT TRACE ELEMENTS
THROUGH A SOIL PROFILE NEAR MT. DAISEN, JAPAN

by

CYNTHIA MARIE JACKSON

Under the Direction of W. Crawford Elliott, Ph.D.

ABSTRACT

After a catastrophic 9.0 magnitude earthquake struck the east coast of Japan in April 2011, a chain of events was set in motion leading to the release of several volatile radionuclides of Cs and I into the atmosphere due to explosions in three of the six reactor cores at the Fukushima-Daiichi Nuclear Power Plant (FDNPP). This study shows the enrichment of stable Cs relative to other alkali metals at the surface soil samples collected from a 1m thick andisol at Mt. Daisen, Japan, roughly 700 Km SW from the FDNPP. Cs is not enriched in three surface soils collected from the Fukushima Prefecture outside the restricted area. The relative enrichment of Cs compared to other alkali metals show the potential of long-term fixation of radiocesium in these Mt. Daisen soils.

INDEX WORDS: Fukushima, Radiocesium, Andisols, Vermiculite

THE GEOCHEMICAL TRENDS OF MAJOR AND SELECT TRACE ELEMENTS
THROUGH A SOIL PROFILE NEAR MT. DAISEN, JAPAN

by

CYNTHIA MARIE JACKSON

A Thesis Submitted in Partial Fulfillment of the Requirements for the Degree of

Master of Science

In the College of Arts and Sciences

Georgia State University

2015

Copyright by
Cynthia Marie Jackson
2015

THE GEOCHEMICAL TRENDS OF MAJOR AND SELECT TRACE ELEMENTS
THROUGH A SOIL PROFILE NEAR MT. DAISEN, JAPAN

by

CYNTHIA MARIE JACKSON

Committee Chair: W. Crawford Elliott

Committee: Nadine Kabengi

Katie Price

Electronic Version Approved:

Office of Graduate Studies

College of Arts and Sciences

Georgia State University

December 2015

ACKNOWLEDGEMENTS

I would like to thank Dr. Crawford Elliott for his tremendous amount of support in completing this thesis. I would also like to thank Dr. Katie Price and Dr. Nadine Kabengi for being on my committee. I thank the Department of Geosciences for the teaching assistantship and stipend which helped enable me to undertake graduate study in Geosciences at Georgia State University.

TABLE OF CONTENTS

ACKNOWLEDGEMENTS	iv
LIST OF TABLES	vii
LIST OF FIGURES	viii
1 INTRODUCTION.....	1
1.1 Events that lead to Disaster	1
<i>1.1.1 The Earthquake, Tsunami and Resulting Devastation</i>	<i>1</i>
<i>1.1.2 Societal Impacts of the Accident at Fukushima.....</i>	<i>3</i>
1.2 Contamination Regions	4
1.3 Vertical Distribution of Cesium in Soils.....	6
1.4 Soils in Japan	9
1.5 Purpose of the Study	10
2 METHODS	11
2.1 Samples Locations and Collection	11
2.2 Major and Trace Elemental Analysis Methods.....	13
<i>2.2.1 Standards and Reproducibility of Major and Select Trace Elements</i>	<i>15</i>
2.3 Data Analysis Methods	15
<i>2.3.1 Calculating Enrichment Factors</i>	<i>15</i>
<i>2.3.2 Pearson's Correlation Coefficient Calculations.....</i>	<i>16</i>
<i>2.3.3 Calculating Molar Ratios</i>	<i>16</i>

3	RESULTS	17
3.1	Results from Major Oxide Analysis	17
3.2	Enrichment Factors of Major Oxides and Select Trace Elements	18
3.2.1	<i>Enrichments Relative to Upper Continental Crust</i>	<i>18</i>
3.2.2	<i>Enrichments Relative to Japanese Andisols</i>	<i>21</i>
3.2.3	<i>Enrichments Relative to Average Loess.....</i>	<i>22</i>
3.3	Molar Ratios	35
4	DISCUSSION	37
4.1	Soil Chemical Profile of Japanese Soils.....	37
4.2	Movement of Radiocesium in the Environment	38
4.3	Potential for Future Studies	40
5	CONCLUSIONS	41
	REFERENCES.....	42
	Appendix A: Data Tables	46

LIST OF TABLES

Table 3-1: Major Oxide Data	17
Table 3-2: Pearson's Correlation Coefficients for Major Element Enrichments Relative to Upper Continental Crust	18
Table 3-3: Major Element Enrichments Relative to Upper Continental Crust.....	19
Table 3-4: Pearson's Correlation Coefficients between Rare Earth Metals	20
Table 3-5: Alkali Metal Enrichments Relative to Upper Continental Crust.....	21
Table 3-6: Table of Calculated Molar Ratios	35

LIST OF FIGURES

Figure 1.1: Diagram of the Up-Dip Motion of the Japan/Pacific Plates.....	1
Figure 1.2: Map of Maximum Water Displacement from Select Tide Gauges	2
Figure 1.3: Emission Rate Timeline for ^{131}I and ^{137}Cs from March 12- March 30	4
Figure 1.4: Distribution of ^{134}Cs and ^{137}Cs near FDNPP.....	5
Figure 1.5: ^{131}I , ^{134}Cs , ^{136}Cs , and ^{137}Cs Spatial Distributions and Ratio of ^{131}I to ^{137}Cs	6
Figure 1.6: Illustration of Chemical Mechanism for which Natural Cesium is Trapped in the Soil	8
Figure 1.7: Vertical Distribution of Radiocesium by Land Use Type.....	8
Figure 1.8: Distribution of allophanic and non-allophanic soils in Japan	10
Figure 2.1: Mt. Daisen Soil Profile (Photo provided by Dr. W. Crawford Elliott)	11
Figure 2.2: Map of Sample Locations Relative to FDNPP and Earthquake Epicenter	13
Figure 3.1: Select Element Composition Enrichments Relative to Upper Continental Crust	23
Figure 3.2: Alkali Metal Enrichments Relative to Upper Continental Crust.....	24
Figure 3.3: Select Alkali and Alkaline Earth Major Element Composition Enrichments Relative to Upper Continental Crust.	25
Figure 3.4: Select Rare Earth Metal Enrichments Compared to Upper Continental Crust	26
Figure 3.5: Major Element Composition Enrichments Relative to Average Japanese Andisols..	27
Figure 3.6: Major Element Composition Enrichments Relative to Average Japanese Andisols..	28
Figure 3.7: Alkali Metal Enrichments Relative to Andisol	29
Figure 3.8: Alkali Metal Enrichments Relative to Andisol	30
Figure 3.9: Major Element Composition Enrichments Relative to Average Loess.....	31
Figure 3.10: Major Element Enrichments Relative to Average Loess	32

Figure 3.11: Alkali Earth Metal Enrichments Relative to Average Loess	33
Figure 3.12: Select Rare Earth Metal Enrichments Relative to Average Loes.....	34
Figure 3.13: Chemical Index of Alteration	36
Figure 4.1: Illustration of the Effect of Radiocesium Sequestration on Root Uptake (Shiozawa, 2013)	40

LIST OF ABBREVIATIONS

FDNPP: Fukushima Daiichi Nuclear Power Plant

TEPCO: Tokyo Electric Power Company

Mw: Moment Magnitude

Bq: Bequerel

Actlabs: Activation Laboratory Ltd.

Cs: Cesium

I: Iodine

NIST: National Institute for Science and Technology

USGS: United States Geological Survey

ICP-MS: Inductive Coupled Plasma Mass Spectrometry

CIA: Chemical Index of Alteration

LOI: Loss on Ignition

UCC: Upper Continental Crust

1 INTRODUCTION

1.1 Events that lead to Disaster

1.1.1 The Earthquake, Tsunami and Resulting Devastation

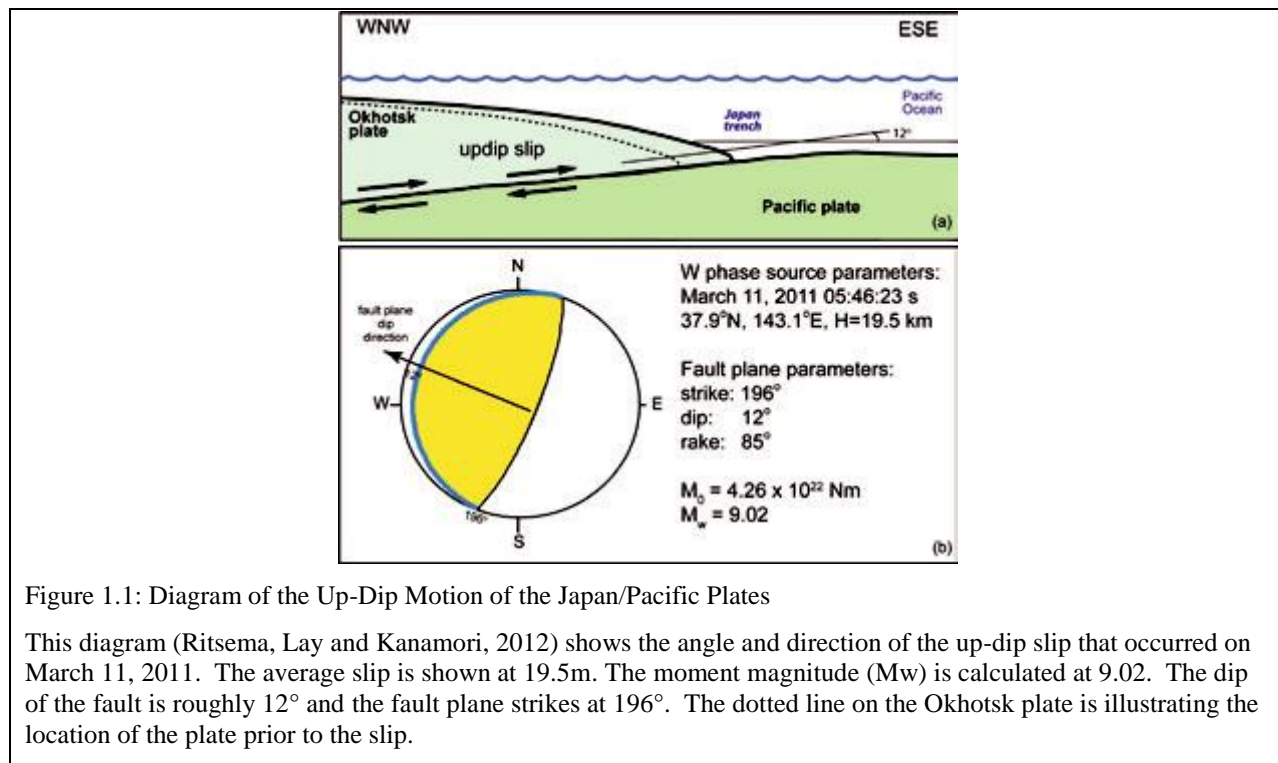


Figure 1.1: Diagram of the Up-Dip Motion of the Japan/Pacific Plates

This diagram (Ritsema, Lay and Kanamori, 2012) shows the angle and direction of the up-dip slip that occurred on March 11, 2011. The average slip is shown at 19.5m. The moment magnitude (M_w) is calculated at 9.02. The dip of the fault is roughly 12° and the fault plane strikes at 196°. The dotted line on the Okhotsk plate is illustrating the location of the plate prior to the slip.

On March 11, 2011, the seafloor ruptured off the northeastern coast of the island of Honshu, Japan resulting in the fourth largest recorded earthquake (Ritsema, Lay and Kanamori, 2012). This earthquake triggered what is now known as a triple disaster that included the damage from the earthquake itself, subsequent tsunami, and finally the explosions at the Fukushima Daiichi nuclear reactors releasing a considerable inventory of radionuclides. The release of these nuclides is still affecting Japan (Bacon and Hobson, 2014). This earthquake occurred on a large megathrust shown in Figure 1.1. The earthquake is the most studied earthquake in the world to date, due to the growth in earthquake monitoring infrastructure since the Kobe earthquake in 1995 (Kawase, 2014).

This earthquake occurred off the coast of the Miyagi-oki area at 2:46 pm (Ritsema, Lay and Kanamori, 2012). The rupture duration lasted for a total of 150 seconds, which is fairly short for a large ($M_w = 9.0$) magnitude earthquake (Kawase, 2014). The magnitude of this earthquake caught many seismologists by surprise, since it is the most intense earthquake in 1100 years based on tsunami deposits and records (Ritsema, Lay and Kanamori, 2012). This rupture happened along the plate boundary between the Pacific Plate and the Okhotsk Plate, ultimately resulting in a tsunami with a height of up to 40 m in some areas (Ritsema, Lay and Kanamori, 2012). The tsunami travelled as far inland as 10 km (Choi et al., 2014). It crashed into the island of Honshu less than 30 minutes after the earthquake (Ritsema, Lay and Kanamori, 2012). The eastward trajectory of the tsunami reached all the way to southern Chile as seen in Figure 1.2 below.

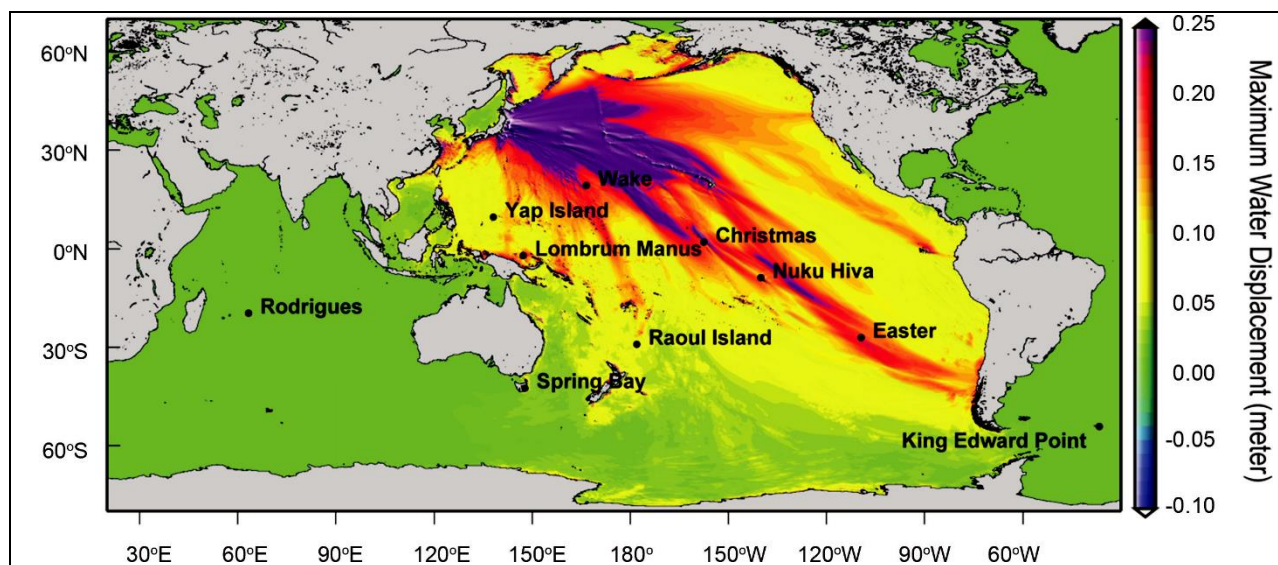


Figure 1.2: Map of Maximum Water Displacement from Select Tide Gauges

The image above (Choi et al., 2014) displays the maximum water displacement from select tidal gauges world wide. Closest to the epicenter of the earthquake, water is displaced upwards of 0.25m. The tsunami reaches as far as the southern tip of South America.

The Fukushima Daiichi Nuclear Power Plant (FDNPP) is located in the Tohoku District on the northeast side of the island of Honshu (Yoshida and Takahashi, 2012). This power plant was the Tokyo Electric Power Company's (TEPCO) first nuclear power plant with Unit 1 becoming functional in 1971 and finally Unit 6 functional in 1979 (Atomic Energy Society of Japan, 2015). The FDNPP contains 6 boiling water reactors. Units 1-4 are located along the coast south of Units 5 and 6 (Blandford and Ahn, 2012). The location of the FDNPP was roughly 155 km from the epicenter of the earthquake. The close proximity made the earthquake powerful enough to damage the circuit breakers leading to a loss of power. However, the earthquake did not affect the safety of the nuclear power reactors at first because the back-up generators restored power to the cooling systems quickly (Atomic Energy Society of Japan, 2015). An hour after the earthquake, the tsunami arrived. The tsunami caused wide spread flooding and damaged many seawater cooling devices. All AC power was cut to Units 1-5. Units 1, 2, and 4 also lost DC power. Debris from the tsunami hindered the transport of new generators and the required generators were too heavy to be helicoptered in (Atomic Energy Society of Japan, 2015).

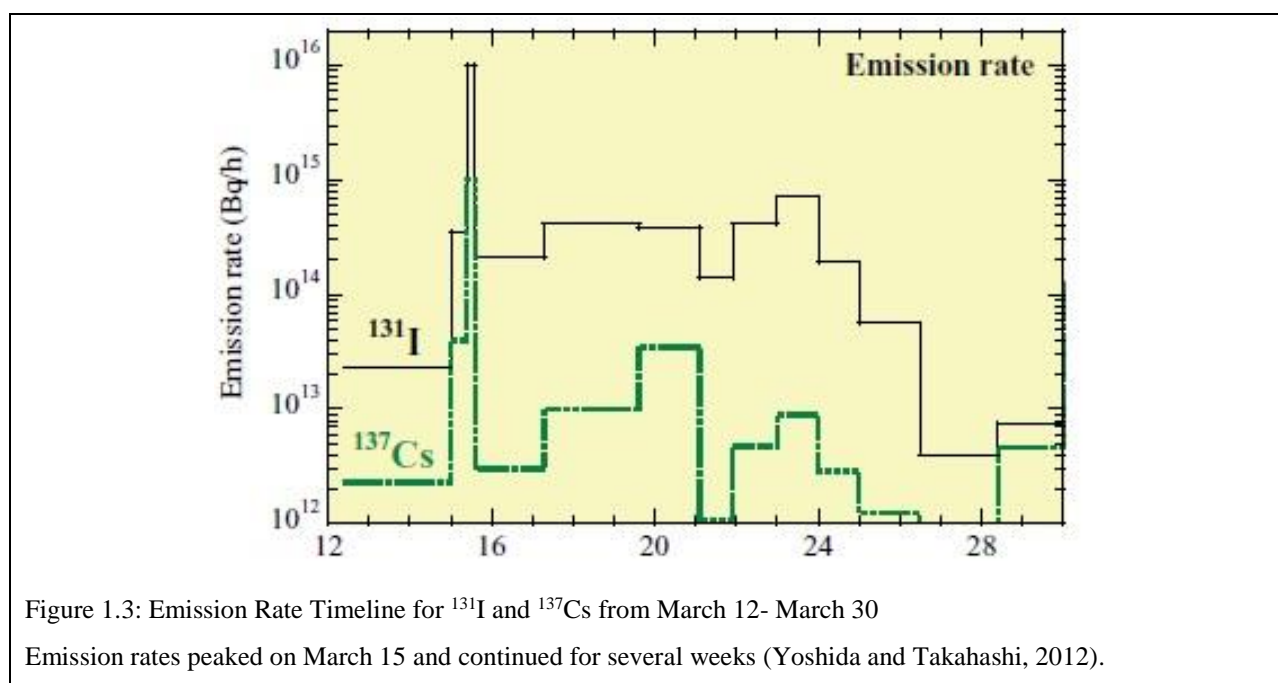
After the power systems failed, the cooling systems also failed (Blandford and Ahn, 2012). On March 12, Unit 1 exploded due to an accumulation of hydrogen from insufficient cooling of the reactor core and fuel rods (Atomic Energy Society of Japan, 2015). The explosion released volatile constituents from the core of the reactors including ^{134}Cs , ^{137}Cs , and ^{131}I , into the environment (Kato, Onda and Teramaga, 2012). The release of transuranic elements is thought to be minimal (Atomic Energy Society of Japan, 2015). Reactors 2-4 likewise exploded after Reactor 1.

1.1.2 Societal Impacts of the Accident at Fukushima

The earthquake and tsunami killed roughly 18,000 people in Japan (Kawase, 2014). The

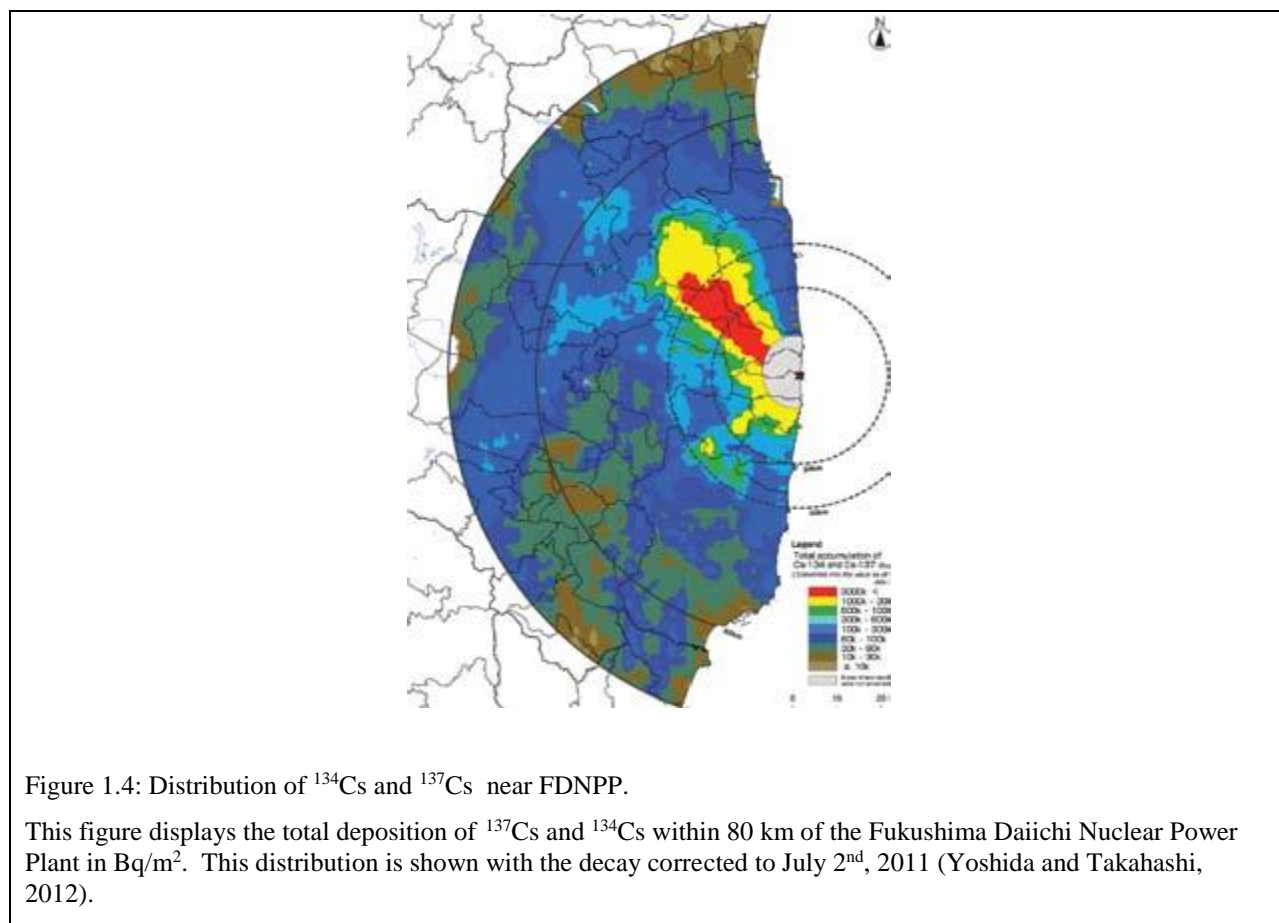
economic losses are estimated at over \$300 billion (Ritsema, Lay and Kanamori, 2012). Japan's building codes and rapid warning systems saved countless lives compared to the 1995 Kobe Earthquake which resulted in the death of 6,000 people, economic losses of over \$100 Billion, and nearly 300,000 people left homeless, despite only having a moment magnitude (Mw) of 6.9 (Chung, 1996). The Tohoku Earthquake in comparison was over 100 times more powerful but only resulted in 3 times the economic losses and lives lost.

1.2 Contamination Regions



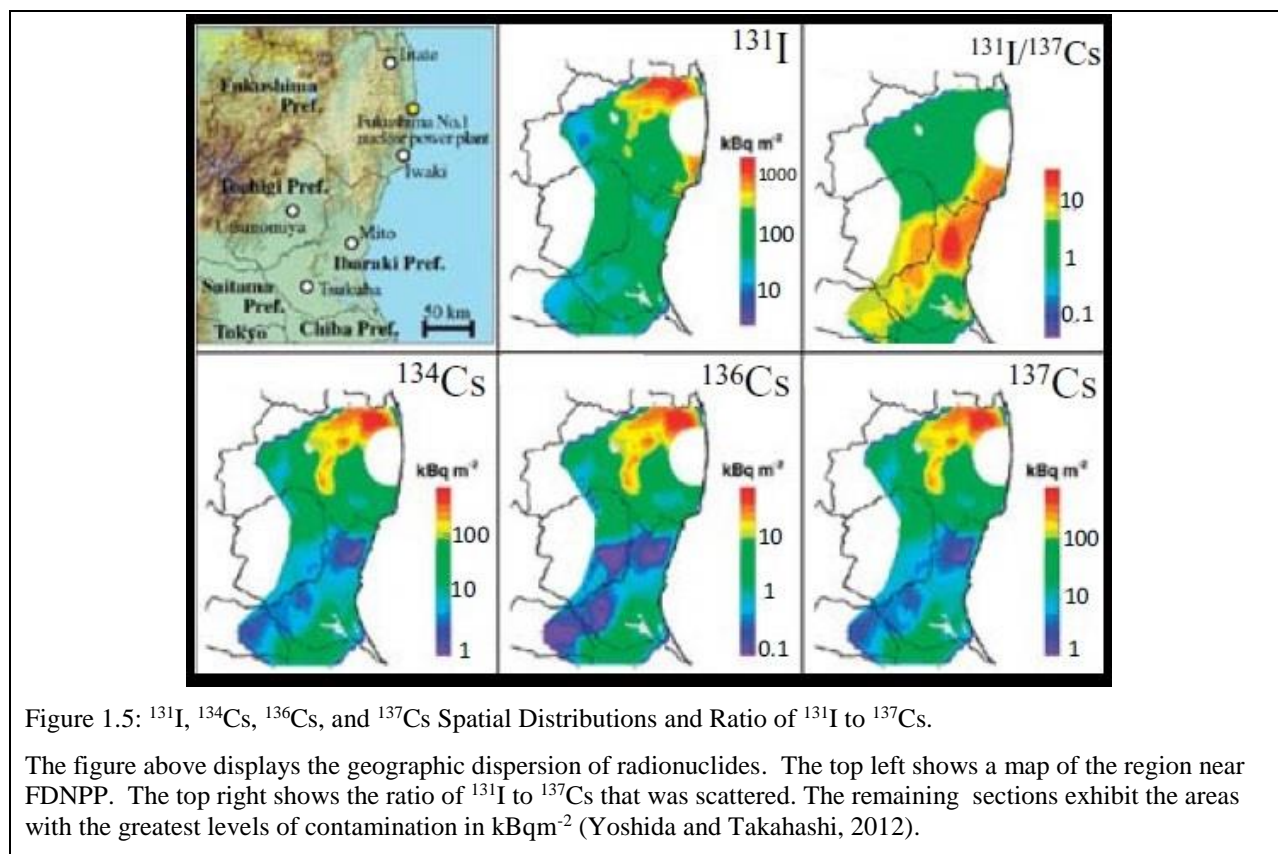
The majority of the radioactive materials released from FDNPP were carried in a northwest trajectory away from the plant between March 12 and April 2011, as seen in Figure 1.4. The FDNPP discharged contaminants including: ^{129}Te , ^{131}I , ^{134}Cs , ^{136}Cs , ^{137}Cs , ^{140}Ba , ^{140}La , and possibly $^{99\text{m}}\text{Tc}$ and ^{110}Ag (Endo et al., 2012). The amounts released were 1.3×10^{16} Bequerel (Bq) of ^{137}Cs and 1.5×10^{16} Bq ^{131}I (Chino et al., 2011). The timeline for the release of these two radionuclides can be seen in Figure 1.3. Only a very low fraction of the reactor core was

released based on the measured ^{237}Pu released from FDNPP (Bossew, 2013) Ambient radioactivity is measured in the soils within the Fukushima Prefecture and the radioactivity of a nearby soil was $0.27 \mu\text{Sv h}^{-1}$ (0.03mR h^{-1} or 0.2Ry^{-1} ; W.C. Elliott, personal communication, 2014). The radiation released from this accident did not reach the Mt. Daisen area.



The radionuclide that is of most interest is ^{137}Cs because it is the volatile radionuclide emitted from the FDNPP with the longest half-life, roughly 30 years. Radioiodine and ^{134}Cs are of less concern at this point since they have half-lives of 8 days and 2 years respectively. Within the first month after the tsunami, approximately 1.3×10^{16} becquerel were expelled and carried to the area northwest of Fukushima (Yoshida and Takahashi, 2012). When Unit 1 exploded on March 12, the prevailing wind was flowing north, limiting contamination to the coastline

(Mathieu et al., 2012). The wind shifted east on March 13 when Unit 3 ruptured. By March 16, the wind had shifted to the west, and Unit 2 exploded (Mathieu et al., 2012). The wind remained toward the west as radioactive debris continued to be discharged from the damaged units for the next several weeks (Mathieu et al., 2012). The majority of ^{137}Cs was emitted from March 15-16 and is displayed in Figure 1.5. ^{131}I is also displayed in the figure, but as it has a half-life of only 8 days it is not considered a long-term hazard.

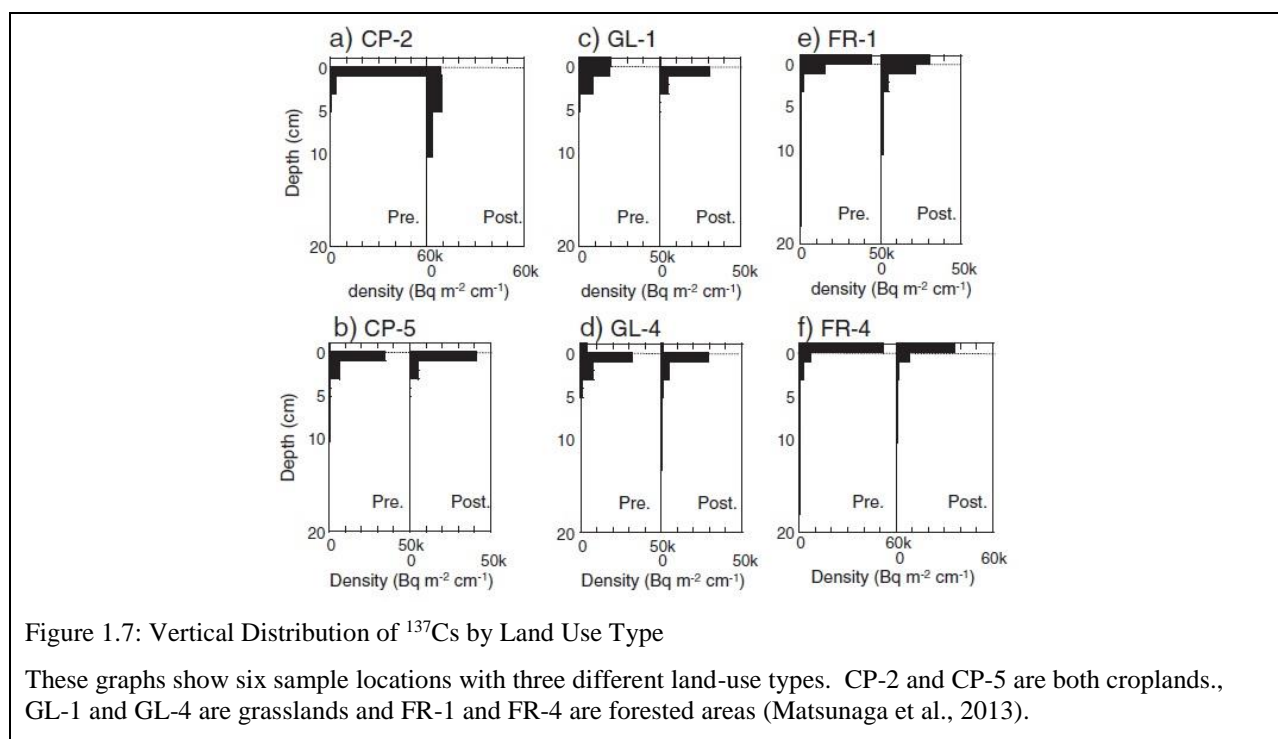
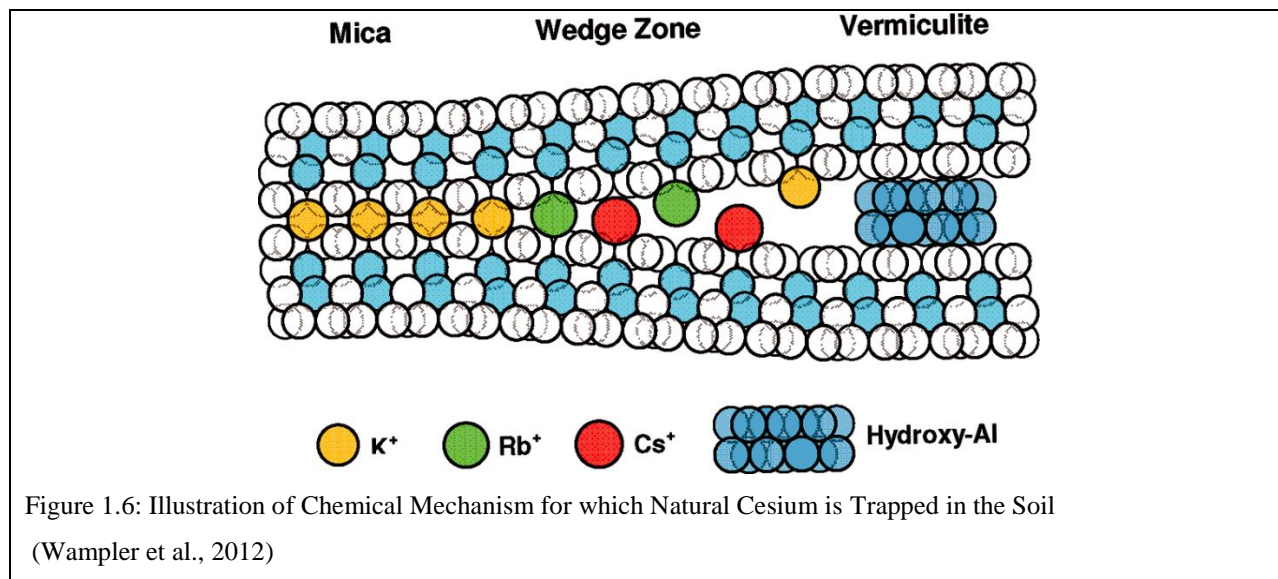


1.3 Vertical Distribution of Cesium in Soils

Since radiocesium (^{137}Cs , ^{134}Cs) exists as a simple ion in water, it was originally thought that the rainy season in Japan would cause the radionuclides to sink deeper into the soil, thus limiting surface exposure (Matsunaga et al., 2013). The monitoring of the concentration of ^{137}Cs as a function of depth was studied before and after the rainy seasons in Japan. This monitoring

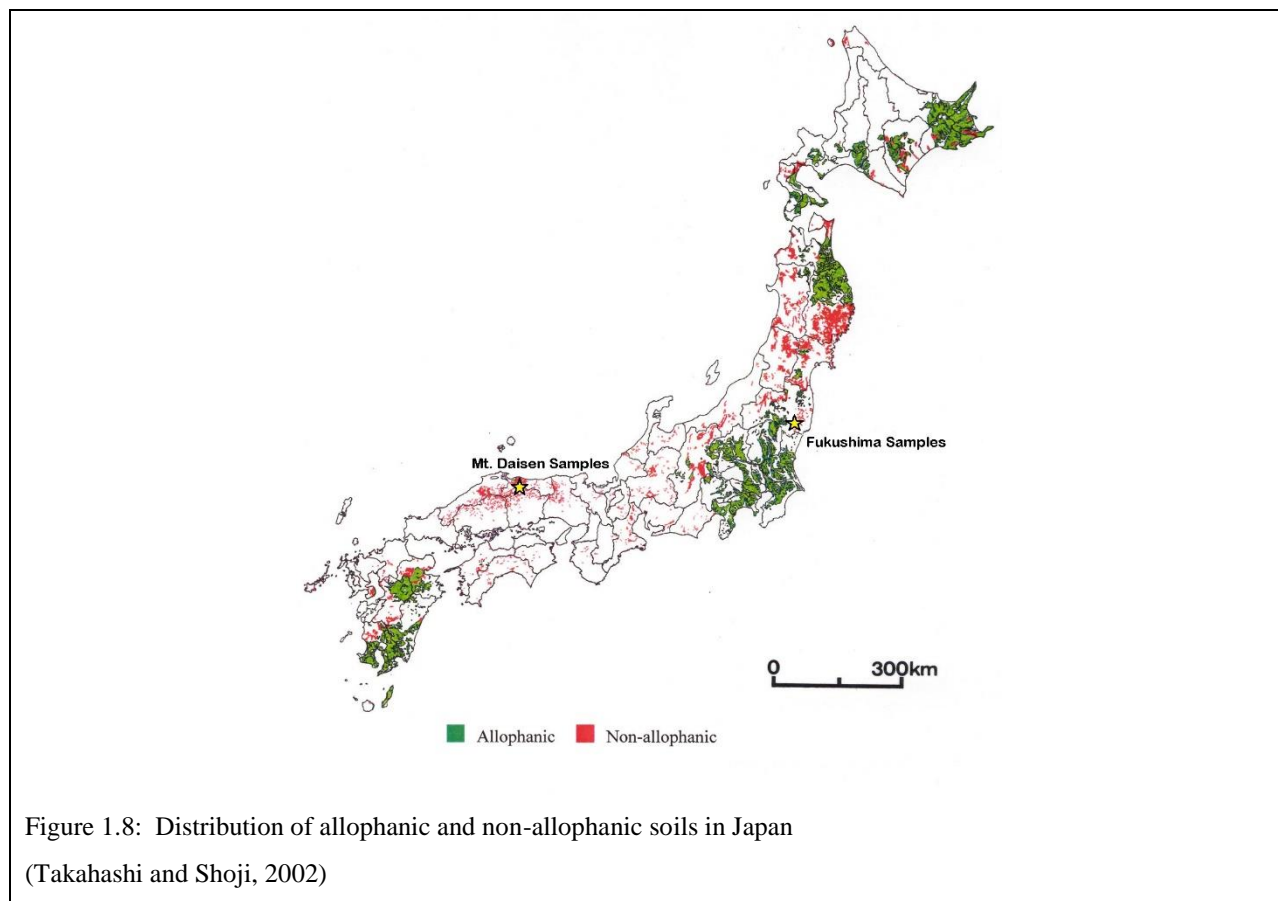
showed that very little of the ^{137}Cs migrated to deeper parts of the soil (Matsunaga et al., 2013). In this study, 15 sample locations were chosen over three different types of environments: croplands, grasslands, and forest. They found ^{137}Cs in the upper 5 cm of these soils (Matsunaga et al., 2013). By taking 20 cm cores, they were able to show that the ^{137}Cs was being sequestered in the top of 5 cm of the soil for all land types (Matsunaga et al., 2013). The reason for the deeper penetration at the sample labeled CP-2, was due to soil tilling after the pre-rainy season sample had been taken (Matsunaga et al., 2013). Despite this, the ^{137}Cs still remained in the top 10 cm of the soil as seen in Figure 1.7: Vertical Distribution of ^{137}Cs by Land Use Type. This strong fixation occurred during the first 2-3 months after the accident (Shiozawa, 2013).

In a study that was published the previous year, the ^{137}Cs sequestration rate in the soil was positively correlated with bulk density, and the content of silt and clay-sized particles (Koarashi et al., 2012). This same study also attributed an increase of organic matter with a decrease of ^{137}Cs retention (Koarashi et al., 2012). These results lead to the idea that Cs was fixed in these soils by phyllosilicate minerals such as illite, vermiculite, smectite. The chemical mechanism behind this fixation is believed to be the result of cesium ions occupying space in the interlayer where potassium ions were once present, as illustrated in Figure 1.7 (Wampler et al., 2012). Natural cesium is interchangeable with radiocesium, making the study of natural cesium important.



1.4 Soils in Japan

Given the projected mineralogical fixation of ^{137}Cs in soils as described in preceding Section 1.3, the mineralogy is important to study to understand the fixation of Cs in these soils. Many of the soils in Japan are composed of andisols, or soils formed from volcanic tephra (Nanzyo, 2007). These soils mostly consist of silicate minerals found in immature or recently formed soils (Soil Survey Staff, 2015). Andisols consist of mostly non-crystalline amorphous minerals. One of these minerals is allophane, a hydrous aluminosilicate mineral. However, the samples that are analyzed in this study represent two regions that contain non-allophanic andisols. These soils have a high exchangeable acidity that are the result of the presence of 2:1 layer silicates (Takahashi and Shoji, 2002). Andisols make up over one-fourth of the agricultural land use in Japan (Figure 1.8), making their remediation a priority after the Fukushima Nuclear Accident (Takahashi and Shoji, 2002).



The region surrounding Mt. Daisen is mountainous and the parent material for the soils is an underlying volcanic tephra (Tsukui, 1984). The soil profile of the region contains a distinct A-horizon that is thick and dark. This A-horizon is rich in clays and consists of less than 25% humus (Harada, 1955). Beneath this A-horizon is a B-horizon that contains a yellow-brown loam (Harada, 1955). The C-horizon is recognizable by its yellow coloring, crystal-rich texture (Kotaki, Katoh and Kitani, 2011), and its increased allophanic content compared to the A-horizon (Harada, 1955).

1.5 Purpose of the Study

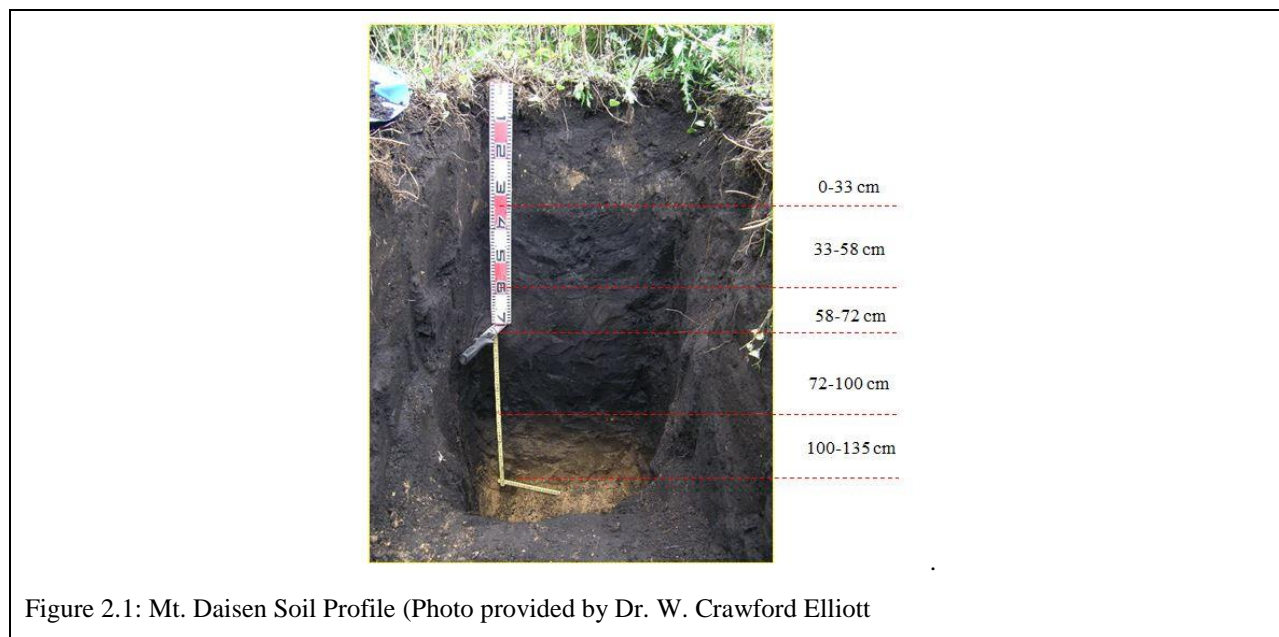
The primary goal of this study is to survey the geochemical (major and select trace element) trends in an andisol not affected by the input of anthropogenic ^{137}Cs from the FDNPP.

Such a survey is useful from a couple of standpoints. Given the accidental release of radionuclides did not affect this soil, a multi-element survey is useful to show elemental trends in andisols not impacted by the accidental release from FDNPP. Secondly, the mobility and fixation of stable Cs in these soils provides a conceptual map for predicting the movement and fixation of ^{137}Cs in an andisol. Stable Cs is a geochemical proxy for radioactive Cs.

2 METHODS

2.1 Samples Locations and Collection

The Mt. Daisen samples and one other set of soils from another locality (not studied) were sent in two containers from Japan. There are approximately 12 samples of no more than 500 grams of soil in each sample. Five soils were from the Mt. Daisen locality. These samples were collected from the top 1.35 meters of this soil down to the parent tephra as seen in Figure 2.1. They are: A-horizon organic soils and C horizon altered weathered volcanic ashes.



A separate B-horizon was not observed. The soils were collected August 7, 2013 by Dr. Elliott, Dr. Atishushi Nakao (Kyoto Prefectural University), and Dr. Atsunobo Kadano (Tottori University of Environmental Studies) from the Mount Daisen region. The location based on GPS data is: N35°22' 42.29", E133°30' 41.29". The soil profile was a meter thick of black soils underlain by weathered tephra. A small amount of tephra was seen in the lower half of this soil. These samples are indicated with a prefix of DS-04 on all graphs and tables.

On September 14, 2014 a separate set of samples were collected near Fukushima Prefecture, Japan. This collection was performed by Dr. Atishushi Nakao and Dr. Crawford Elliott. Sample 14-1 was collected at N37°38.753'' and E140°30.998' at a depth of about 15-25 cm. This sample was located on a hilltop in an undisturbed forest. Granite float was observed near this site. Sample 14-2 was collected at N37°46.313' E140°29.917'. The soil at this second site was an open field covered in grass and Persimmon roots. Sample 14-2 was collected at a depth of 15-25 cm. The radiation at the surface near sample 14-2 was measured at $0.12 \mu\text{Svhr}^{-1}$ ($\sim 0.01 \text{ mRhr}^{-1}$) (W.C. Elliott, personal communication, 2014). A third sample of alluvial soil was collected from the Fukushima Prefecture from the Kyoto Prefecture University soil collection archives by Prof. Nakao and Prof. Junta Yanai (Kyoto Prefecture University, sample # Yanai (0701P)). This archived sample was collected prior to 2011. Sample locations are shown in Figure 2.2.

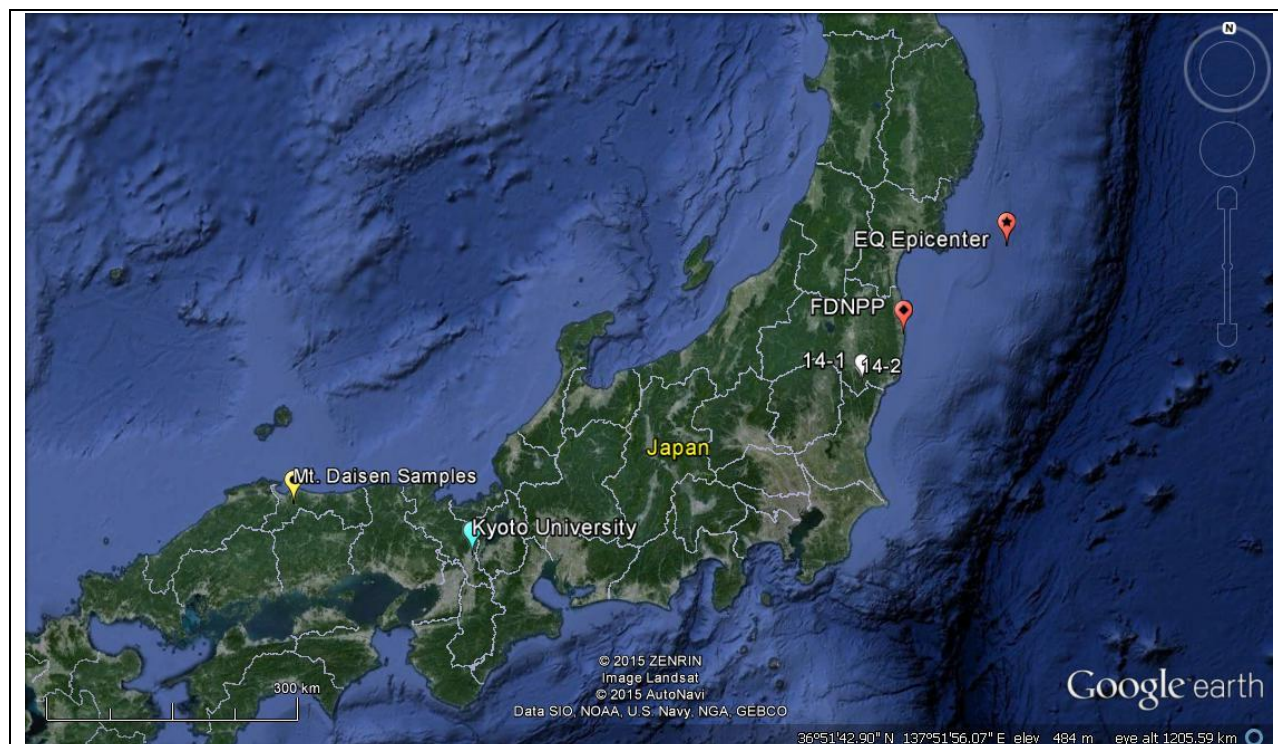


Figure 2.2: Map of Sample Locations Relative to FDNPP and Earthquake Epicenter.

Source: Google Earth

2.2 Major and Trace Elemental Analysis Methods

Representative bulk samples were produced by splitting the sample received into four subsamples. Representative samples of the subsamples from the Mt. Daisen and Fukushima were sent to Activation Laboratory Ltd. in Ancaster, Canada for major and select analyses of trace elements. A variety of methods were used by Activation Laboratory Ltd (hereinafter Actlabs): inductively coupled plasma-mass spectrometry (ICP-MS) and Instrumental Neutron Activation Analysis (INAA). The major element samples were prepared by combining 0.2g of the sample with a mixture of lithium metaborate/lithium tetraborate. The mixture was fused in a graphite crucible. The fused liquid/glass was then dissolved into a 5% nitric acid solution. After the glass was dissolved, these analytes were analyzed using a Varian Vista ICP for major elements and select trace elements. Major element oxides were calculated from the metal concentrations using

standard gravimetric factors for each element. Loss on ignition (LOI) indicates the percentage of loss on ignition. LOI occurs when the samples are heated to 900°C, which causes the loss of all hydrous portions of the soil as well as the loss of carbons and organics. Control standards were also run and are discussed later.

Alkali, Alkali Earth (Cs, Rb, Sr, Ba) and selected trace elements were analyzed by digesting 0.25g of sample with four acids (HF, HNO₃, HClO₄, HCl), starting with hydrofluoric acid. After hydrofluoric acid was added, the sample was added to a mixture of nitric and perchloric acids for further dissolution. The resulting liquid was then heated using programmed ramping and holding cycles. After heating, the samples were heated to dryness in air to form nitrate, perchlorate and chloride salts. These salts were dissolved using hydrochloric acid. This analyte was then analyzed using a Varian Vista ICP.

Several elements were analyzed using Instrumental Neutron Activation Analysis (INAA) following method by Hoffman (1992). One gram of sample was loaded in a polyethylene vial. The vial, sample and flux wires (monitors or irradiation) were then irradiated at a thermal neutron flux of $7 \times 10^{12} \text{ n cm}^{-2} \text{ s}^{-1}$. The samples were removed and decayed for a 7- day period, to allow Na- 24 to decay. The samples were counted on a high purity Ge detector with resolution of better than 1.7 KeV for the 1332 KeV Co- 60 photopeak. The decay was corrected using the flux wires. The measured activities were compared to a calibration developed from multiple certified international reference materials. The standard present is only a check on accuracy and is not used for calibration purposes. From 10- 30% of the samples were rechecked by re-measurement. For values exceeding the upper limits, assays were recommended. One standard is run for every 11 samples. One blank was analyzed per work order.

2.2.1 Standards and Reproducibility of Major and Select Trace Elements

Actlabs measured many certified interlaboratory reference standards including those from the National Institute for Science and Technology (NIST) and the United States Geological Survey (USGS) for this study. Interlaboratory standards DNC-1, W-2a, SY-4, and BIR-1a are reference samples created by the United States Geological Survey. GBW 07113 is a rhyolite standard material from Brammer Standard Company, Inc. (Houston, TX). NIST 694, DNC-1, W-2a, SY-4, BIR-1a, and GBW 07113 were all used to test the accuracy and precision of the major elements in the soil: SiO₂, Al₂O₃, Fe₂O₃, MnO, MgO, CaO, Na₂O, K₂O, TiO₂, and P₂O₅. These are all interlaboratory standards that are certified and widely accepted in the scientific community. For all major constituents, the standards and duplicate measurements of the samples were within acceptable ranges as judged by agreement with standards and by the totals wt. percent being between 98.5 and 101.5 Wt. %.

2.3 Data Analysis Methods

2.3.1 Calculating Enrichment Factors

Enrichment factors (EF) were calculated to compare concentrations with average upper continental crust compositions (Yanagi, 2011), average Japanese andosol compositions (Takeda et al., 2004), and average Loess compositions (Meyers et al., 1987). Enrichments of select major elements and select trace elements were plotted with respect to depth for the Mt. Daisen soil and for the three bulk samples of the soils collected from the Fukushima Prefecture. The calculation of Enrichment Factor for a given element X is given below (Birkeland, 1994).

$$EF_X = \frac{[X_{sample}]}{[X_{standard}]}$$

Equation 2-1: Calculation for Enrichment Factors.

An enrichment factor of less than 1 indicates a depletion of that element in the soil relative to concentration of that element in a given standard. An EF value of greater than 1 indicates an enrichment of that element in that soil relative to the concentration of that element in a given standard. The line between enrichment and depletion is indicated in each figure by a bold black line labeled “Unity.” The standard typically used is average upper continental crust, average Japanese andisol or average loess as described above.

2.3.2 Pearson’s Correlation Coefficient Calculations

A Pearson’s Correlation Coefficient is a statistic measuring the linear interdependence between two variables or two sets of data. A value of $r=1$ indicates a perfect positive correlation, and a value of $r= -1$ indicates a negative correlation. For this study, a strong correlation is defined as $|r| > 0.9$. Pearson correlation values were calculated between UCC enrichments of major elements, and between select rare earth metals (Cs, Rb, Sr, Ba, Nb, Pb, Th, U, Zr, and La).

$$r = \frac{\sum_i (x_i - \bar{x})(y_i - \bar{y})}{\sqrt{\sum_i (x_i - \bar{x})^2} \sqrt{\sum_i (y_i - \bar{y})^2}}$$

Equation 2-2: Equation for Pearson’s Correlation Coefficient

2.3.3 Calculating Molar Ratios

Molar ratios of select major element oxides were calculated to derive indexes of weathering (SA and CIA). The molar values were derived by dividing the measured percentage oxide by the molar weight of that oxide. SA is the molar ratio of $\text{SiO}_2/\text{Al}_2\text{O}_3$ (Birkeland, 1994). The Chemical Index of Alteration (Nesbitt and Young, 1982) is described below. For CaO^* , this amount is corrected for the amount (if any) of CaO in carbonate phases. The amounts of CaO are < 0.50 wt percent for the soils in this study, thus no correction was needed for the amount of Ca associated

with carbonate in these bulk samples of these soils. Calcite was not observed in bulk diffraction scans of these samples. These soils were not formed in arid environments.

$$SA = \frac{SiO_2}{Al_2O_3}$$

$$CIA = \left[\frac{Al_2O_3}{Al_2O_3 + CaO + Na_2O + K_2O} \right] * 100$$

Equation 2-3: Equations for SA Ratio and CIA.

3 RESULTS

3.1 Results from Major Oxide Analysis

Table 3-1: Major Oxide Data

Samples	Date	SiO ₂	Al ₂ O ₃	Fe ₂ O ₃	TiO ₂	P ₂ O ₅	MnO	MgO	CaO	Na ₂ O	K ₂ O	LOI	Total
DS-04 0-33cm	21-Mar-2014	42.15	15.71	4.19	0.453	0.21	0.061	1.39	2.02	1.73	1.02	29.09	98.03
DS-04 33-58cm	21-Mar-2014	42.93	13.09	3.4	0.35	0.16	0.048	0.89	1.86	1.86	1.14	33.04	98.77
DS-04 58-72cm	21-Mar-2014	45.17	14.85	3.78	0.406	0.14	0.058	1.04	1.94	2.01	1.17	27.87	98.42
DS-04 72-100cm	21-Mar-2014	31.55	13.8	4.25	0.516	0.21	0.045	0.99	1.13	0.91	0.69	45.11	99.2
DS-04 72-100cm	7-Nov-2014	31.9	13.37	4.45	0.49	0.21	0.048	1.02	1.21	0.96	0.68	44.66	98.99
DS-04 72-100cm	11-Feb-2015	34.01	14.89	4.74	0.558	0.21	0.048	1.12	1.31	1.1	0.82	42.03	100.8
DS-04 100-135cm	21-Mar-2014	49.23	19.89	5.41	0.618	0.1	0.065	1.79	1.67	1.52	1.21	18.93	100.4
DS-04 100-135cm	7-Nov-2014	49.55	20.05	5.37	0.609	0.11	0.065	1.8	1.58	1.53	1.3	18.24	100.2
DS-04 100-135cm	11-Feb-2015	50.26	20.72	5.46	0.628	0.24	0.063	1.79	1.55	1.67	1.33	17.21	100.9
DS-04 100-135cm	25-Feb-2015	49.8	20.82	5.52	0.638	0.21	0.065	1.79	1.58	1.56	1.29	16.99	100.3
Fukushima a 14-1	7-Nov-2014	56.08	16.91	7.84	0.938	0.06	0.103	2.36	2.37	1	1.09	10.45	99.19
Fukushima a 14-2	7-Nov-2014	48.11	18.05	10.39	0.983	0.29	0.202	3.23	2.76	1.03	0.68	13.54	99.27
Yanai(0701P)	11-Feb-2015	60.23	15.62	5.73	0.723	0.24	0.085	1.34	2.09	1.55	1.48	9.92	99.01

Actlabs returned the chemical analysis of the data in the form of oxides. Data in the table above is in the form of percentages of the total weight. LOI was highest in the upper portions of

the Mt. Daisen sample. It decreased by half when the parent tephra is reached at 100 cm. The amount of LOI of the Fukushima samples was more lower compared to the Mount Daisen samples.

3.2 Enrichment Factors of Major Oxides and Select Trace Elements

3.2.1 Enrichments Relative to Upper Continental Crust

The relative enrichments of major element compositions are compared to upper continental crust values per Yanagi (2011). These values are tabulated in Table 3-3 and are plotted with respect to sample number and depth in Figure 3.1. This graph shows that there are depletions in all major elements except for Fe_2O_3 . An increase in Fe_2O_3 results from chemical weathering in an oxidizing environment (Birkeland, 1984). Pearson's Correlation Coefficients were calculated using excel and are shown in Table 3-2. There is a strong linear correlation between Fe_2O_3 and TiO_2 . Titanium dioxide is likewise, an insoluble element oxide during chemical weathering in an oxidizing environment. There is also a strong correlation between Fe_2O_3 and MnO as well as Fe_2O_3 and MgO (Table 3-2). Enrichment peaks in Fe_2O_3 , MgO and TiO_2 were found in the Fukushima samples (Figures 3.1 and 3.3). SiO_2 , CaO , Na_2O , and K_2O show relative depletions in all samples (Figure 3.1 and 3.3).

Table 3-2: Pearson's Correlation Coefficients for Major Element Enrichments Relative to Upper Continental Crust

	Al_2O_3	Fe_2O_3	TiO_2	P_2O_5	MnO	MgO	CaO	Na_2O	K_2O
SiO_2	0.57	0.463	0.563	-0.217	0.414	0.526	0.636	0.349	0.775

Al ₂ O ₃	0.418	0.45	-0.087	0.268	0.615	0.148	0.166	0.494
Fe ₂ O ₃		0.955	0.184	0.941	0.952	0.703	-0.465	-0.16
TiO ₂			0.075	0.823	0.891	0.616	-0.506	-0.023
P ₂ O ₅				0.306	0.076	0.022	-0.144	-0.292
MnO					0.889	0.822	-0.301	-0.201
MgO						0.704	-0.29	-0.035
CaO							0.12	0.126
Na ₂ O								0.704

Table 3-3: Major Element Enrichments Relative to Upper Continental Crust

Samples	Date	SiO ₂	Al ₂ O ₃	Fe ₂ O ₃	TiO ₂	P ₂ O ₅	MnO	MgO	CaO	Na ₂ O	K ₂ O
Standard	-	65.20	15.60	2.10	0.60	0.20	0.10	2.30	4.70	3.10	3.30
DS-04 0-33cm	21-Mar-2014	0.65	1.01	2.00	0.76	1.05	0.61	0.60	0.43	0.56	0.31
DS-04 33-58cm	21-Mar-2014	0.66	0.84	1.62	0.58	0.80	0.48	0.39	0.40	0.60	0.35
DS-04 58-72cm	21-Mar-2014	0.69	0.95	1.80	0.68	0.70	0.58	0.45	0.41	0.65	0.35
DS-04 72-100cm	21-Mar-2014	0.48	0.88	2.02	0.86	1.05	0.45	0.43	0.24	0.29	0.21
DS-04 72-100cm	7-Nov-2014	0.49	0.86	2.12	0.82	1.05	0.48	0.44	0.26	0.31	0.21
DS-04 72-100cm	11-Feb-2015	0.52	0.95	2.26	0.93	1.05	0.48	0.49	0.28	0.35	0.25
DS-04 100-135cm	21-Mar-2014	0.76	1.28	2.58	1.03	0.50	0.65	0.78	0.36	0.49	0.37
DS-04 100-135cm	7-Nov-2014	0.76	1.29	2.56	1.02	0.55	0.65	0.78	0.34	0.49	0.39
DS-04 100-135cm	11-Feb-2015	0.77	1.33	2.60	1.05	1.20	0.63	0.78	0.33	0.54	0.40
DS-04 100-135cm	25-Feb-2015	0.76	1.33	2.63	1.06	1.05	0.65	0.78	0.34	0.50	0.39
Fukushima 14-1	7-Nov-2014	0.86	1.08	3.73	1.56	0.30	1.03	1.03	0.50	0.32	0.33
Fukushima 14-2	7-Nov-2014	0.74	1.16	4.95	1.64	1.45	2.02	1.40	0.59	0.33	0.21
Yanai (0701P)	11-Feb-2015	0.92	1.00	2.73	1.21	1.20	0.85	0.58	0.44	0.50	0.45

Table 3-5, shows the calculated relative enrichments of alkali elements (Cs, Rb, Sr, Ba) and select rare earth metals (Nb, Pb, Th, U, Zr, and La) compared to upper continental crust values per Yanagi (2011). The enrichment factors of the alkali elements are graphed in Figure 3.2. Natural cesium is enriched at all soil depths relative to upper continental crust in the Mt. Daisen samples. A large enrichment is seen in DS 72-100 cm, Mt. Daisen (Figure 3.2). The

Table 3-5: Alkali Metal Enrichments Relative to Upper Continental Crust

Samples	Date	Ba	Cs	Rb	Sr	Nb	Pb	Th	U	Zr	La
Standard	-	550.00	3.70	112.00	350.00	25.00	20.00	10.70	2.80	190.00	30.00
DS-04 0-33cm	21-Mar-2014	0.42	1.57	0.49	0.80	0.42	0.90	0.82	1.00	0.68	0.89
DS-04 33-58cm	21-Mar-2014	0.47	1.43	0.55	0.80	0.36	0.95	0.70	0.86	0.53	0.82
DS-04 58-72cm	21-Mar-2014	0.50	1.43	0.52	0.89	0.37	1.00	0.75	0.86	0.53	0.97
DS-04 72-100cm	21-Mar-2014	0.29	2.46	0.63	0.42	0.59	0.75	1.22	1.42	0.63	1.80
DS-04 72-100cm	7-Nov-2014	0.29	1.30	0.30	0.43	0.13	0.50	0.55	0.64	0.30	0.94
DS-04 72-100cm	11-Feb-2015	0.30	1.38	0.36	0.55	0.32	0.60	2.02	1.76	1.44	1.76
DS-04 100-135cm	21-Mar-2014	0.47	1.49	0.54	0.73	0.34	0.60	0.78	0.78	0.69	0.51
DS-04 100-135cm	7-Nov-2014	0.49	1.57	0.54	0.67	0.37	0.45	0.76	0.73	0.74	0.52
DS-04 100-135cm	11-Feb-2015	0.51	2.03	0.52	0.73	0.37	1.10	25.23	6.11	1.98	15.87
DS-04 100-135cm	25-Feb-2015	0.49	1.59	0.51	0.75	0.37	0.00	24.67	5.82	1.82	15.93
Fukushima 14-1	7-Nov-2014	0.48	0.89	0.47	0.31	0.26	0.40	0.39	0.38	0.81	0.50
Fukushima 14-2	7-Nov-2014	0.54	0.38	0.30	0.52	0.17	0.25	0.21	0.38	0.56	0.33
Yanai (0701P)	11-Feb-2015	0.69	0.95	0.48	0.40	0.32	0.90	3.53	1.98	1.22	2.33

3.2.2 Enrichments Relative to Japanese Andisols

In Figure 3.5, the relative enrichments of major element compositions are compared to average Japanese andisols per Takeda et al. (2004). This figure paints a different picture than the one indicated with Figure 3.2 by showing relative depletions in all major elements for all samples, except for Na_2O , which was enriched in the Mt. Daisen samples (Figure 3.6). Figure 3.5 also contradicts the Fe_2O_3 enrichments that were seen in Figure 3.1. The alkali metals (Cs, Rb, Sr) show enrichments relative to Japanese Andisols while Ba is depleted in Figure 3.7. The Fukushima samples show a depletion of natural cesium, which is similar to the data normalized to Upper Continental Crust (Figure 3.2). Figure 3.8 displays similar trends in enrichments as seen in Figure 3.4. Data tables for andisol enrichment factors can be found in the Appendix.

3.2.3 *Enrichments Relative to Average Loess*

Enrichment factors for major oxides were calculated compared to average loess as per (Zhang et al., 2013). These enrichments are displayed in Figures 3.9 and 3.10. Figure 3.9 highlights enrichment in Al_2O_3 for all samples when compared to average Chinese loess. Compared to loess, the Fukushima samples show enrichments in all major oxides, aside from SiO_2 , MgO , Na_2O , and K_2O (Figures 3.9 and 3.10). Enrichments in natural cesium compared to loess as per normalization per Taylor & McLennan (1985) shown in Figure 3.11, are consistent with the enrichment trends relative to upper Continental Crust that were seen in Figures 3.2 and 3.7. Figure 3.12 displays trends that are similar to those seen in Figures 3.8 and 3.4. Data tables for loess enrichment factors can be found in the Appendix.

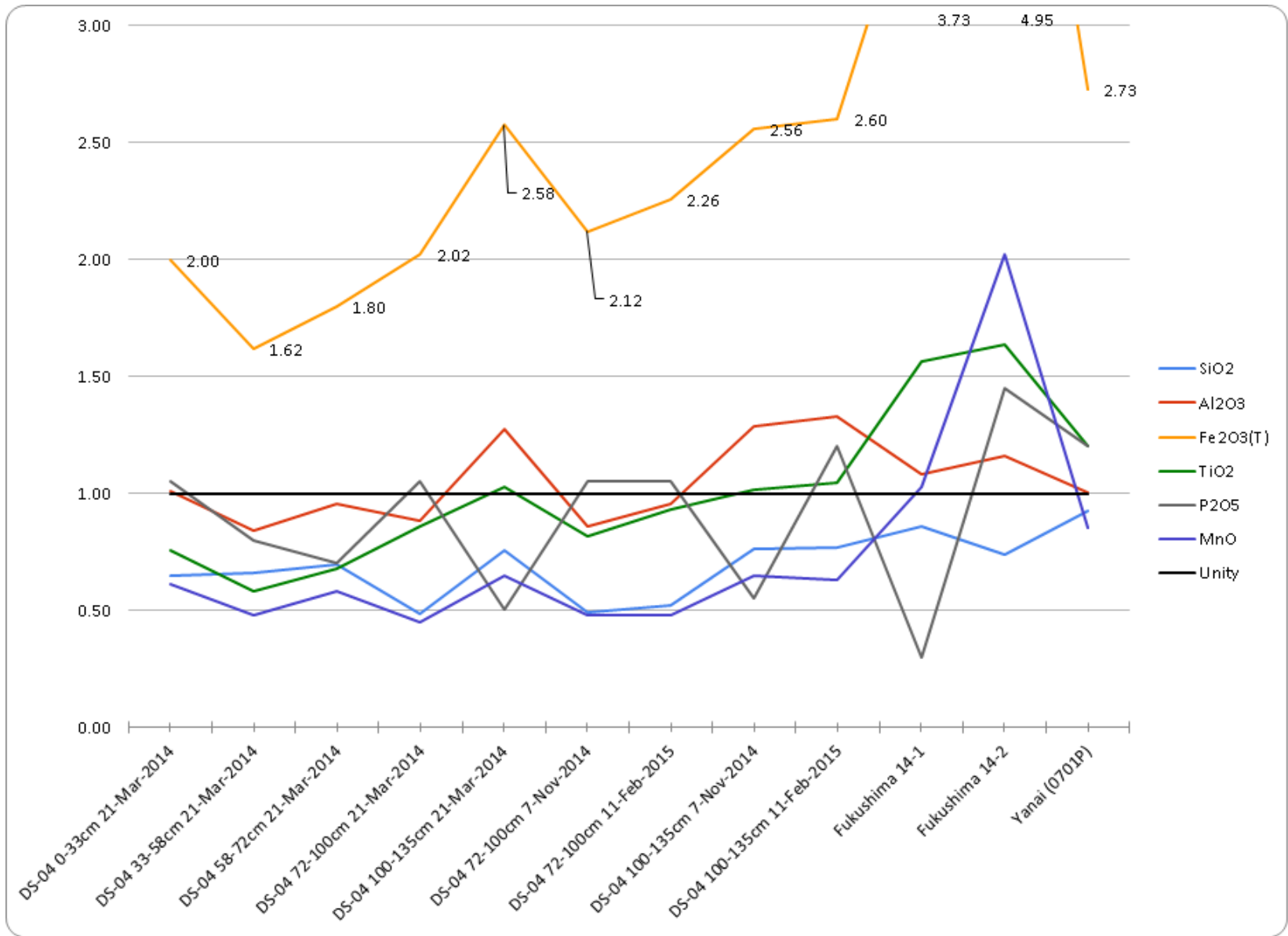


Figure 3.1: Select Element Composition Enrichments Relative to Upper Continental Crust

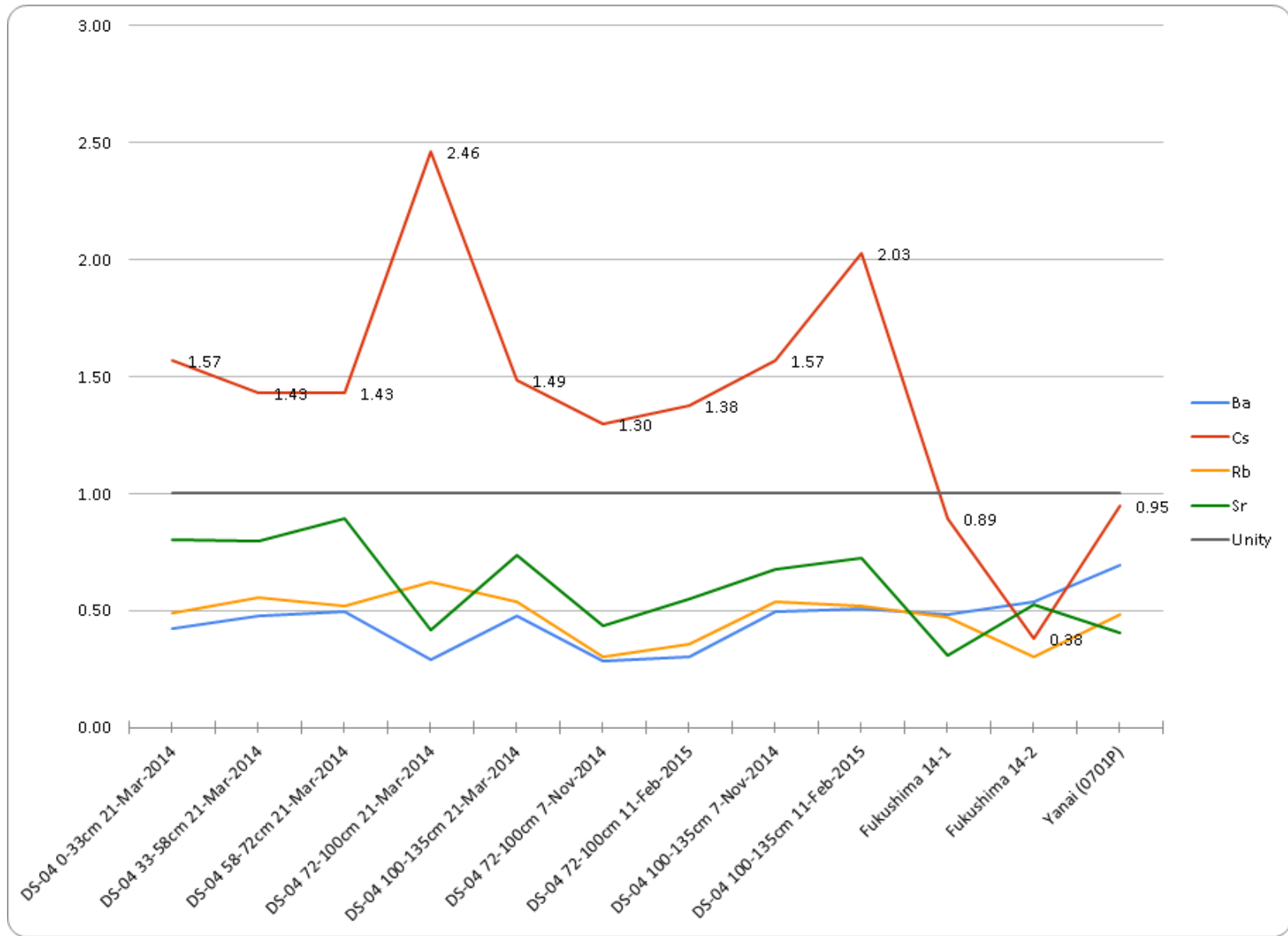


Figure 3.2: Alkali Metal Enrichments Relative to Upper Continental Crust

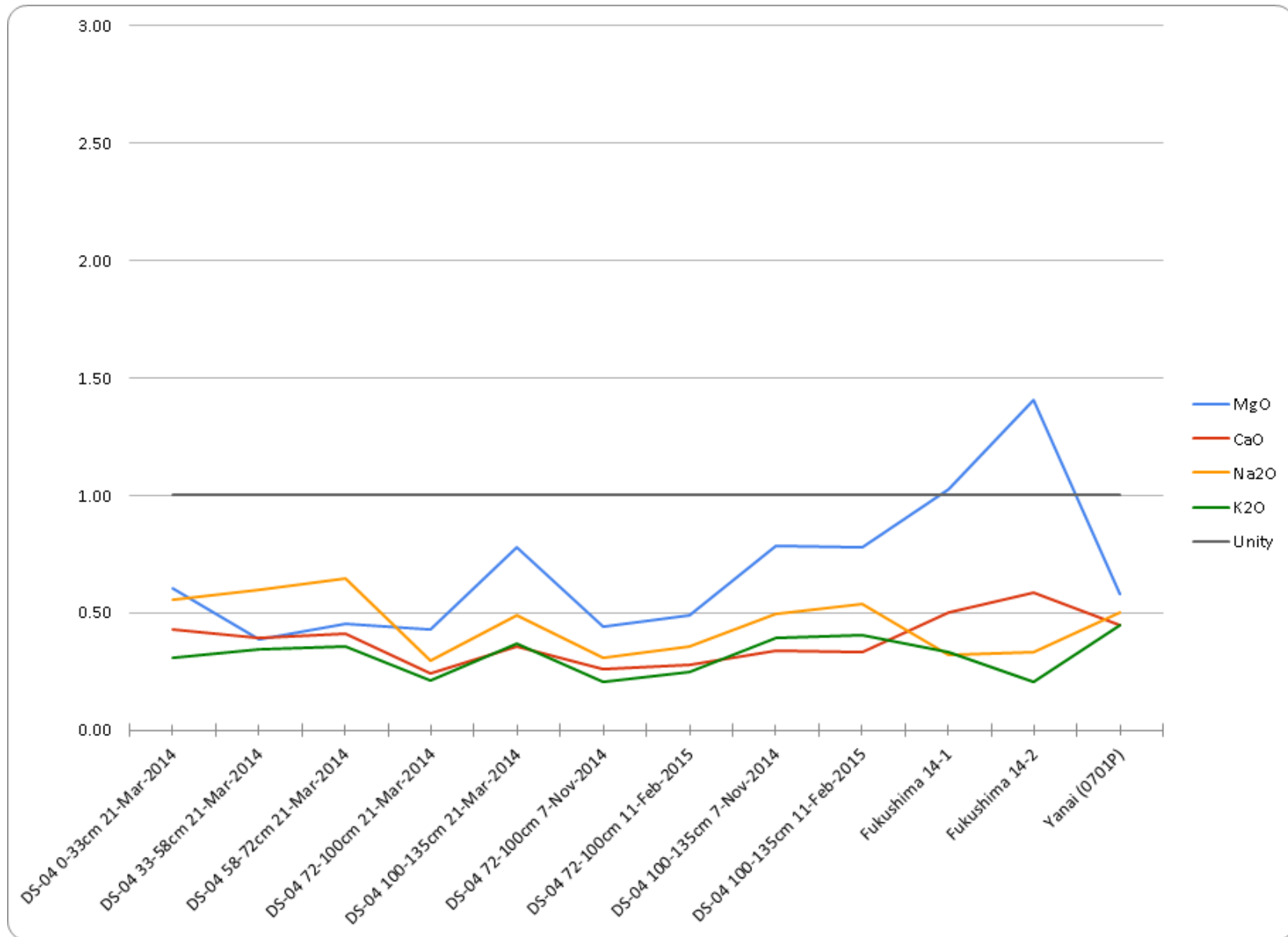


Figure 3.3: Select Alkali and Alkaline Earth Major Element Composition Enrichments Relative to Upper Continental Crust.

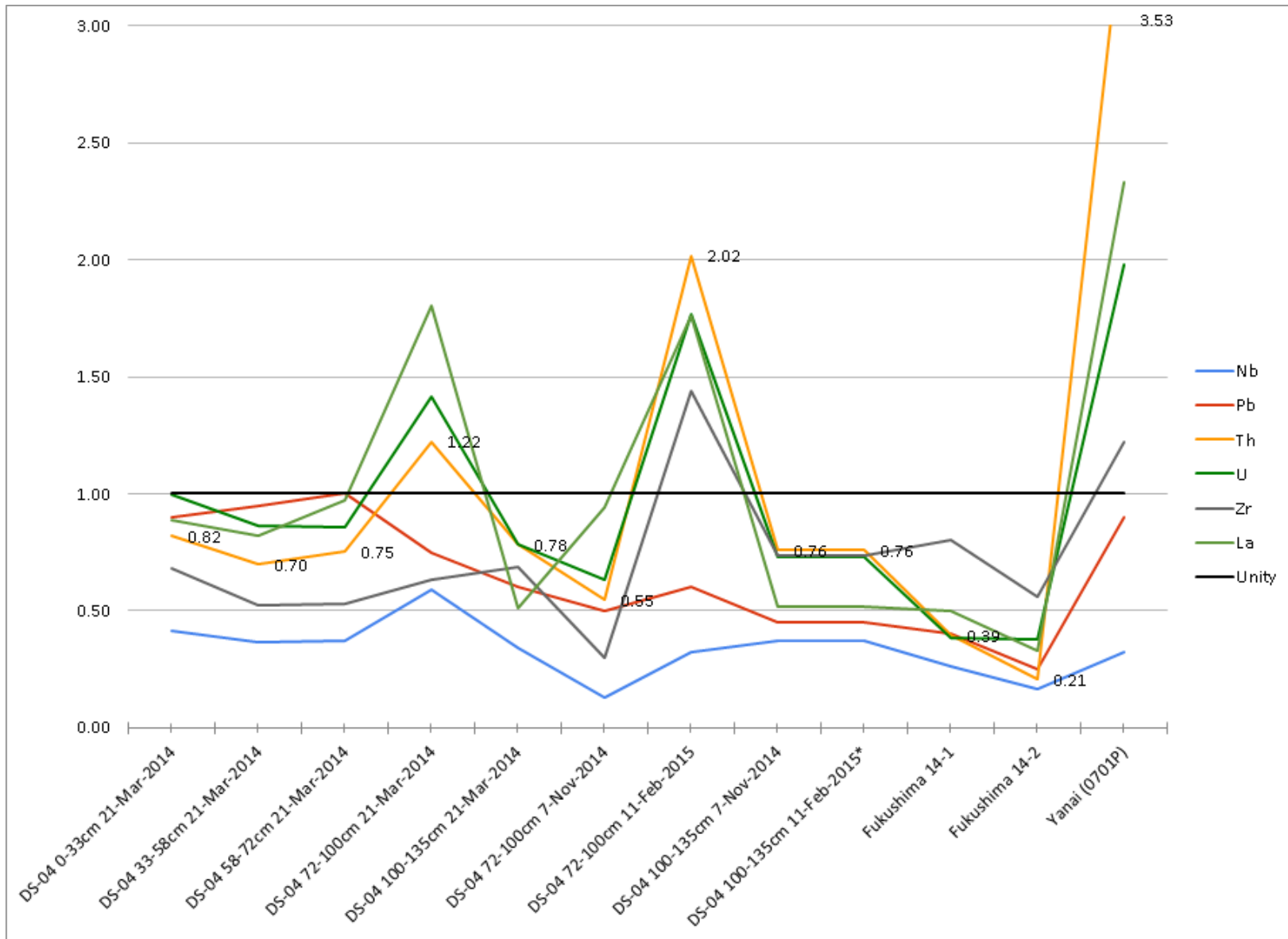


Figure 3.4: Select Rare Earth Metal Enrichments Compared to Upper Continental Crust.

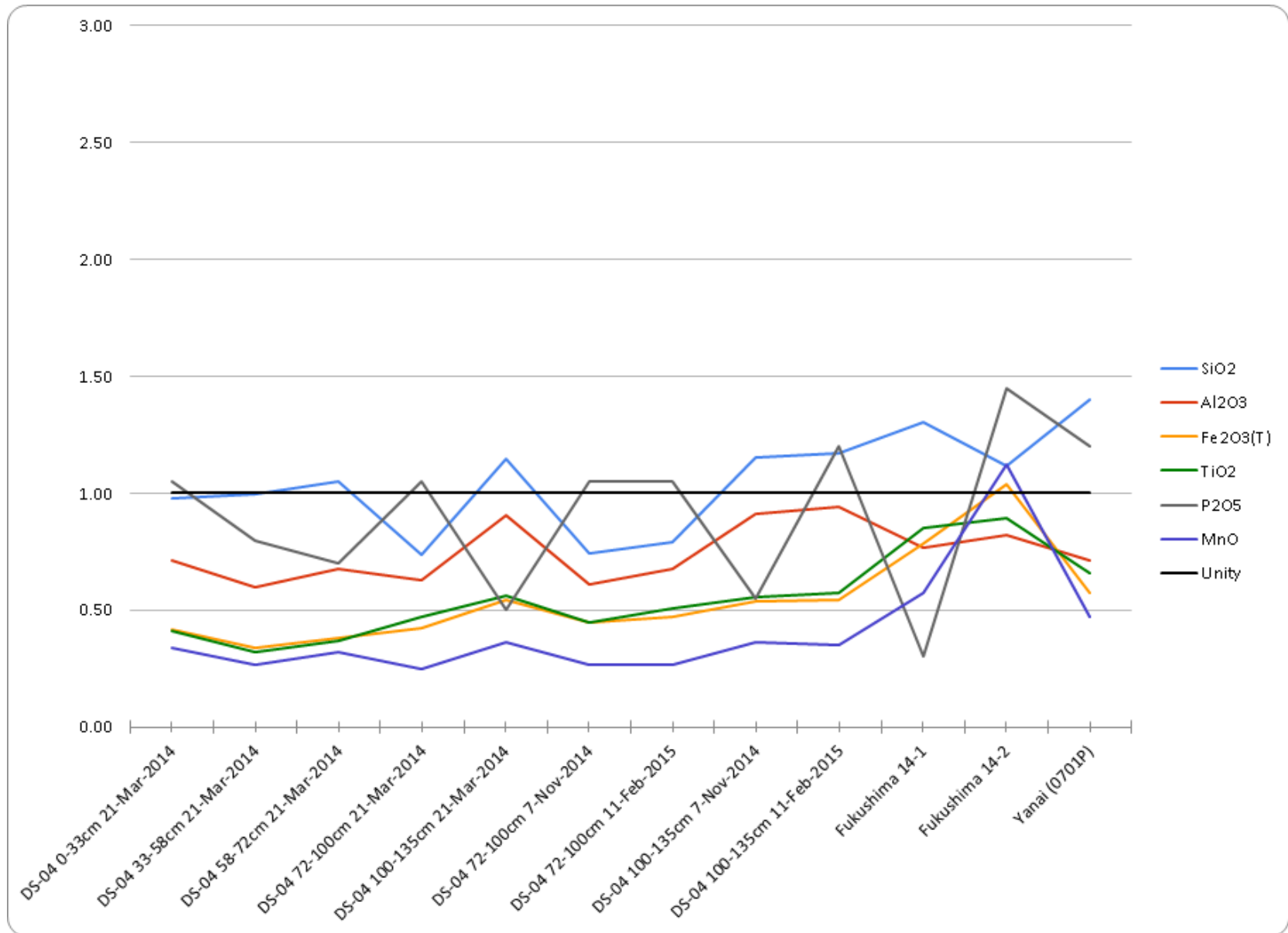


Figure 3.5: Major Element Composition Enrichments Relative to Average Japanese Andisols.

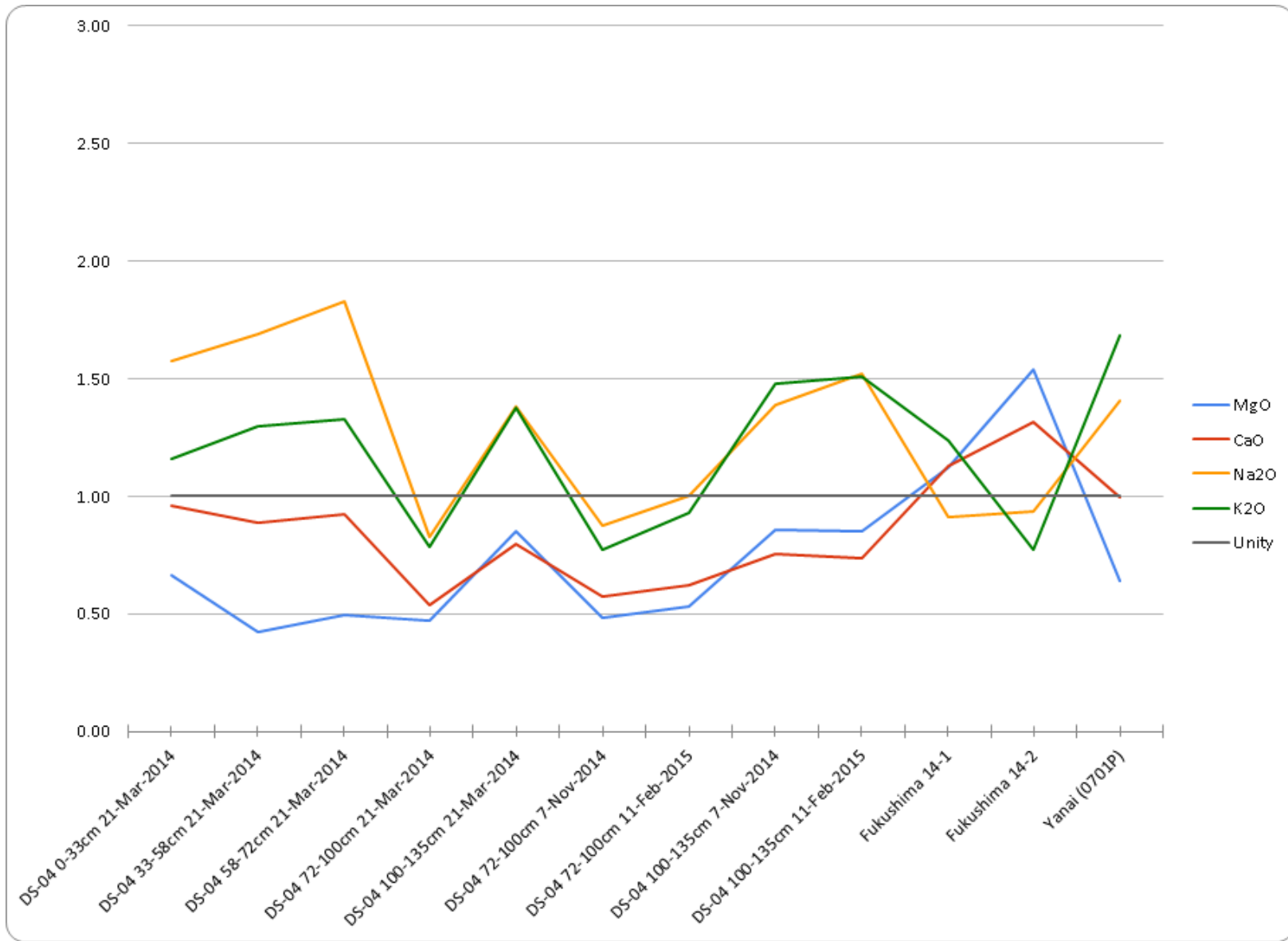


Figure 3.6: Major Element Composition Enrichments Relative to Average Japanese Andisols.

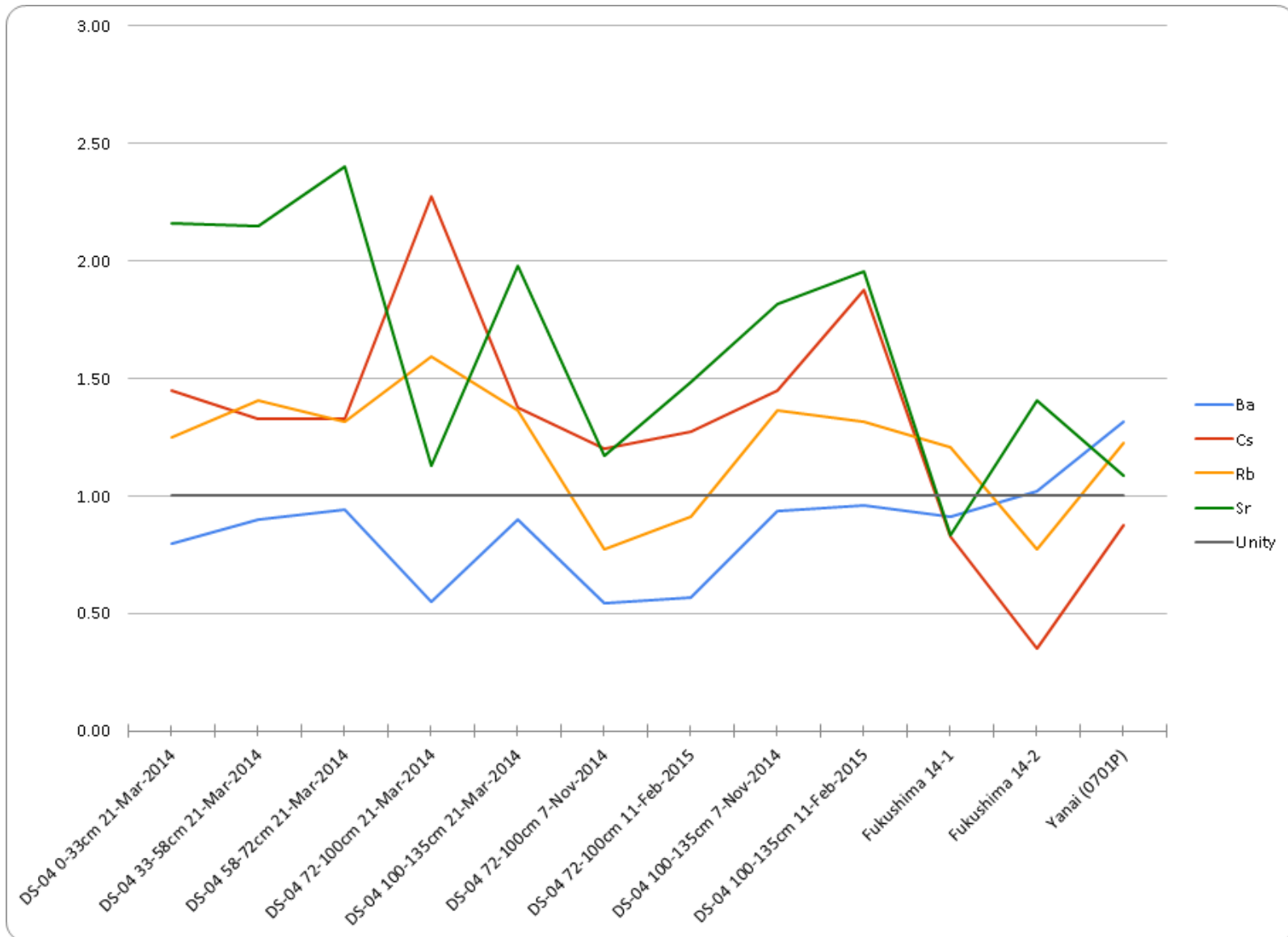


Figure 3.7: Alkali Metal Enrichments Relative to Andisol.

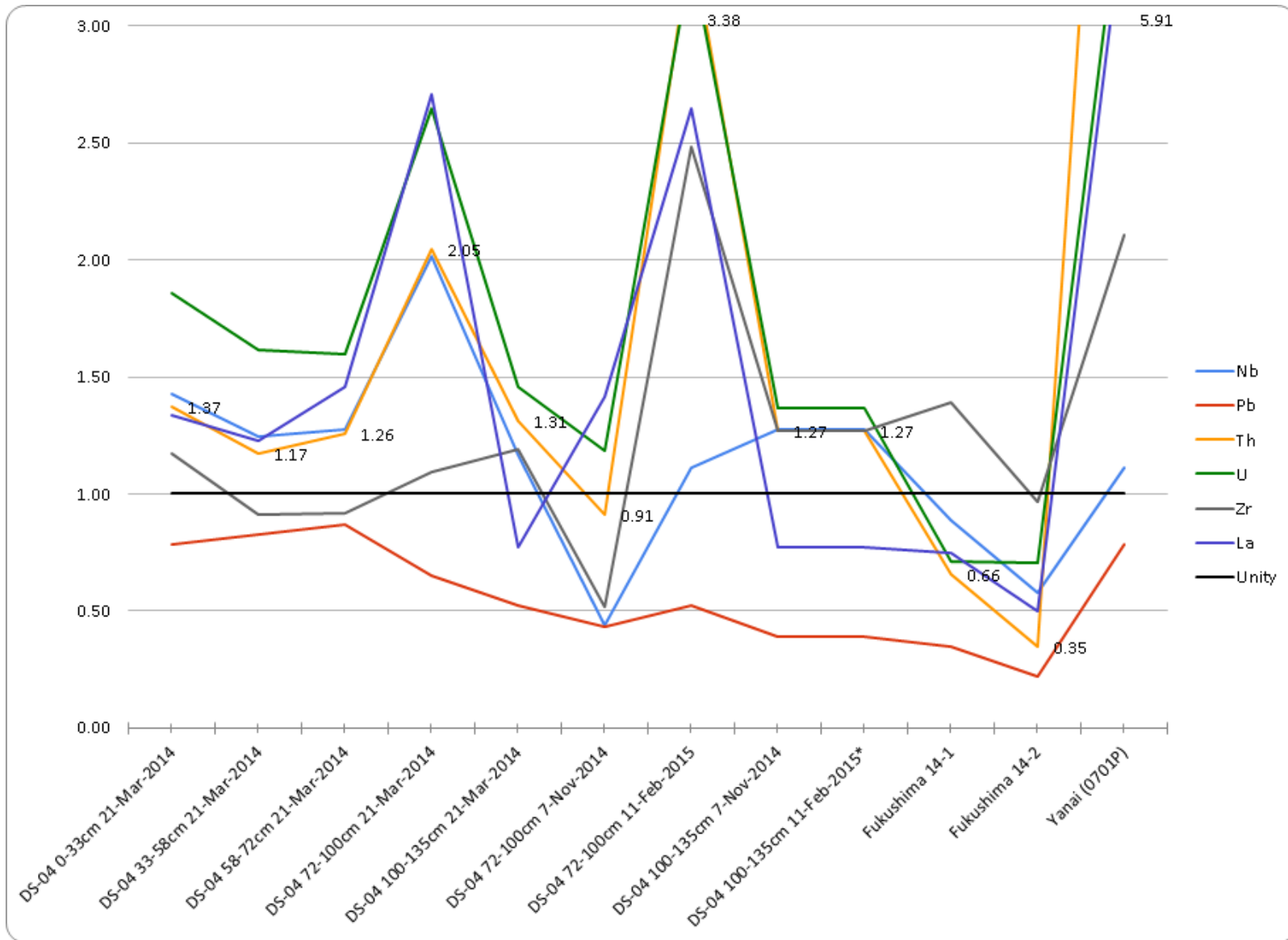


Figure 3.8: Alkali Metal Enrichments Relative to Andisol.

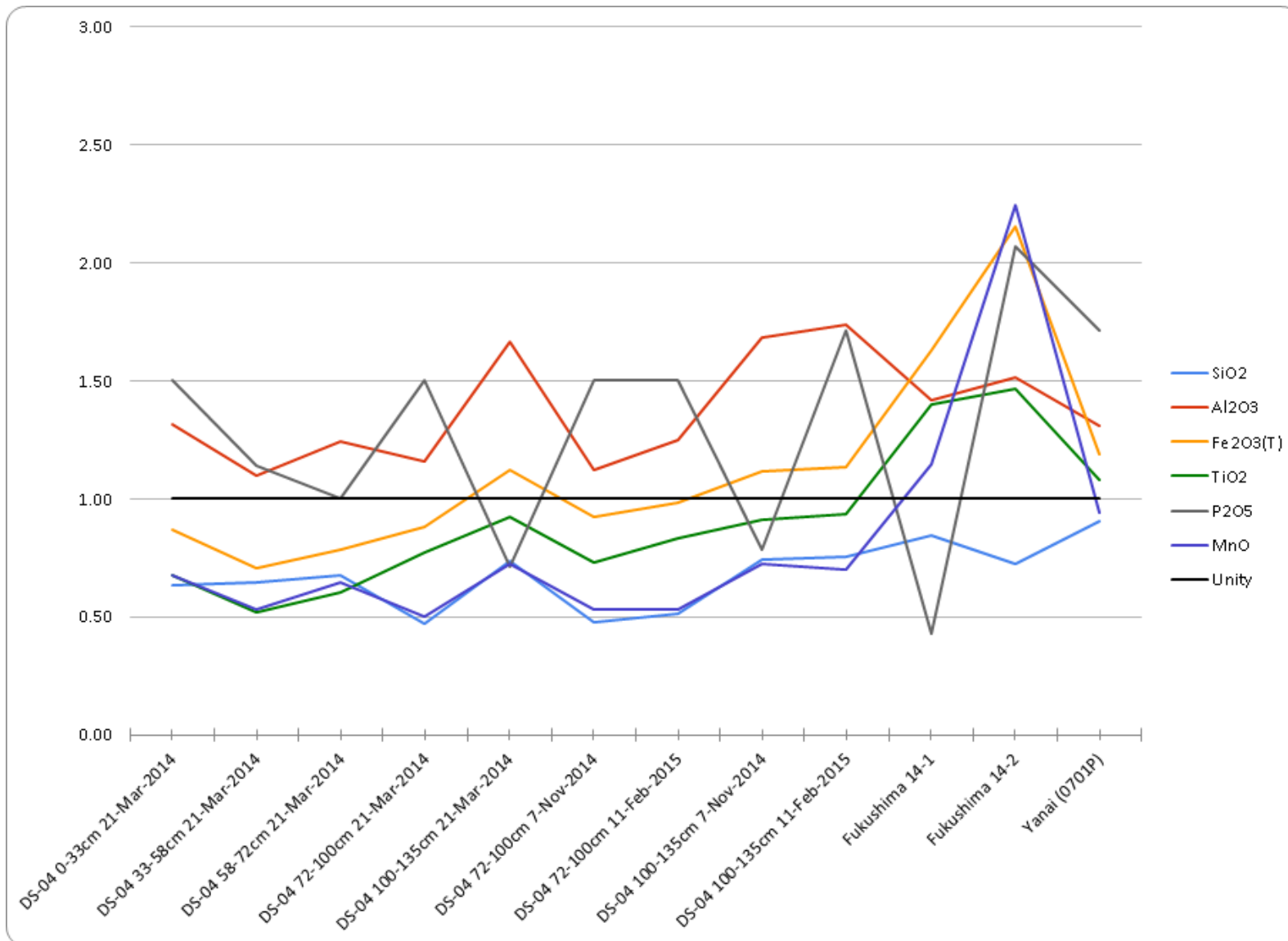


Figure 3.9: Major Element Composition Enrichments Relative to Average Loess.

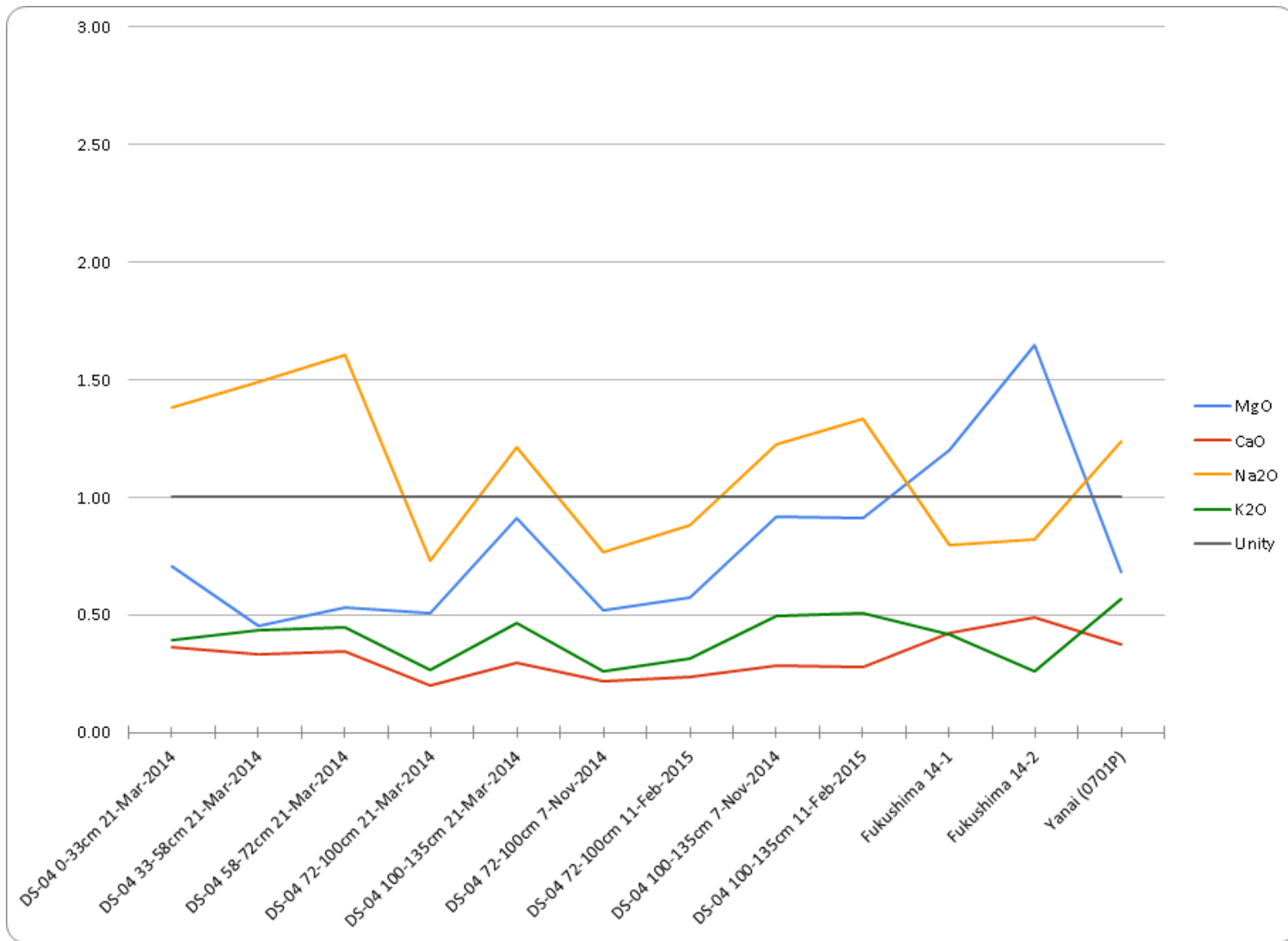


Figure 3.10: Major Element Enrichments Relative to Average Loess.

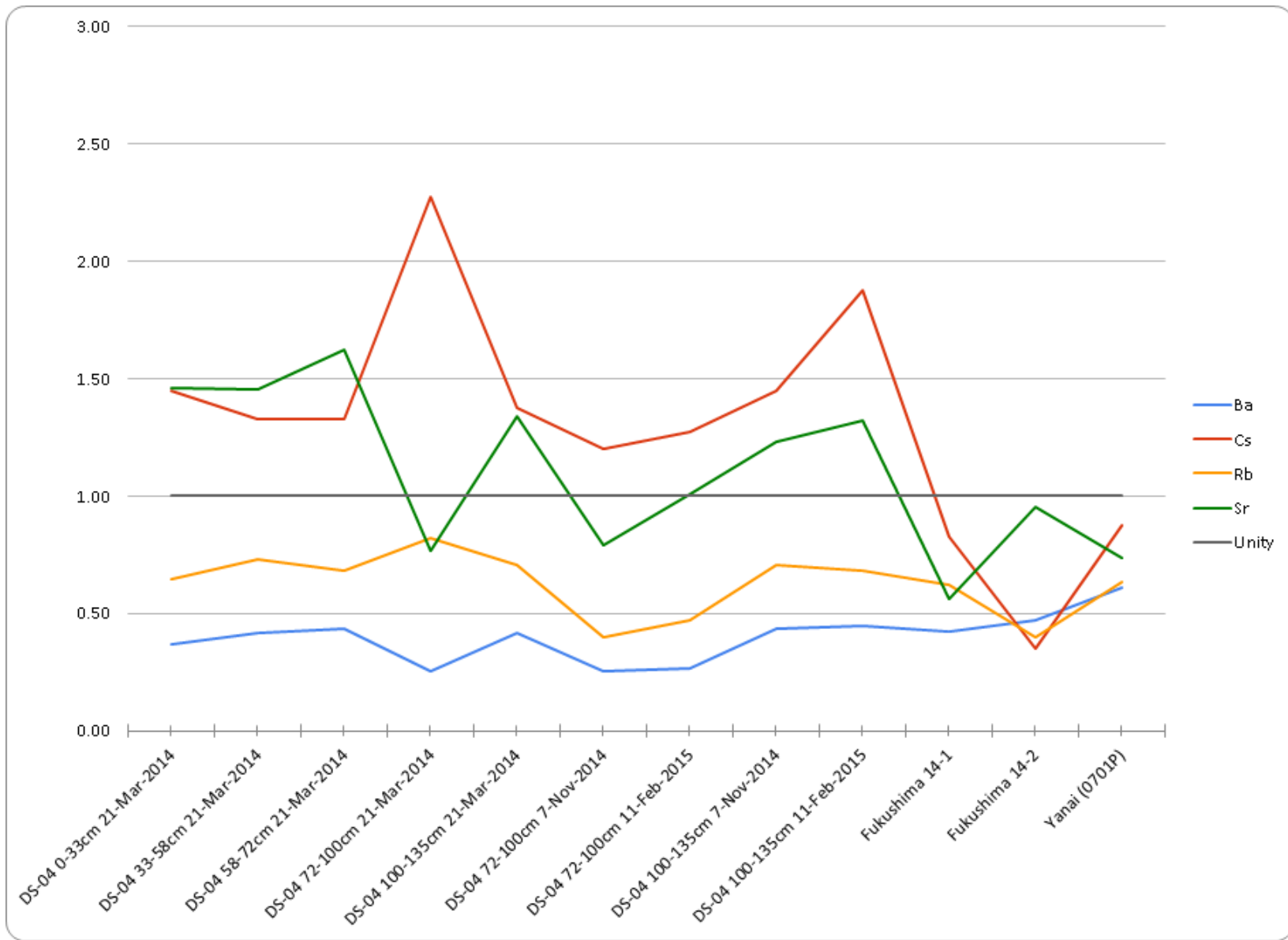


Figure 3.11: Alkali Earth Metal Enrichments Relative to Average Loess.

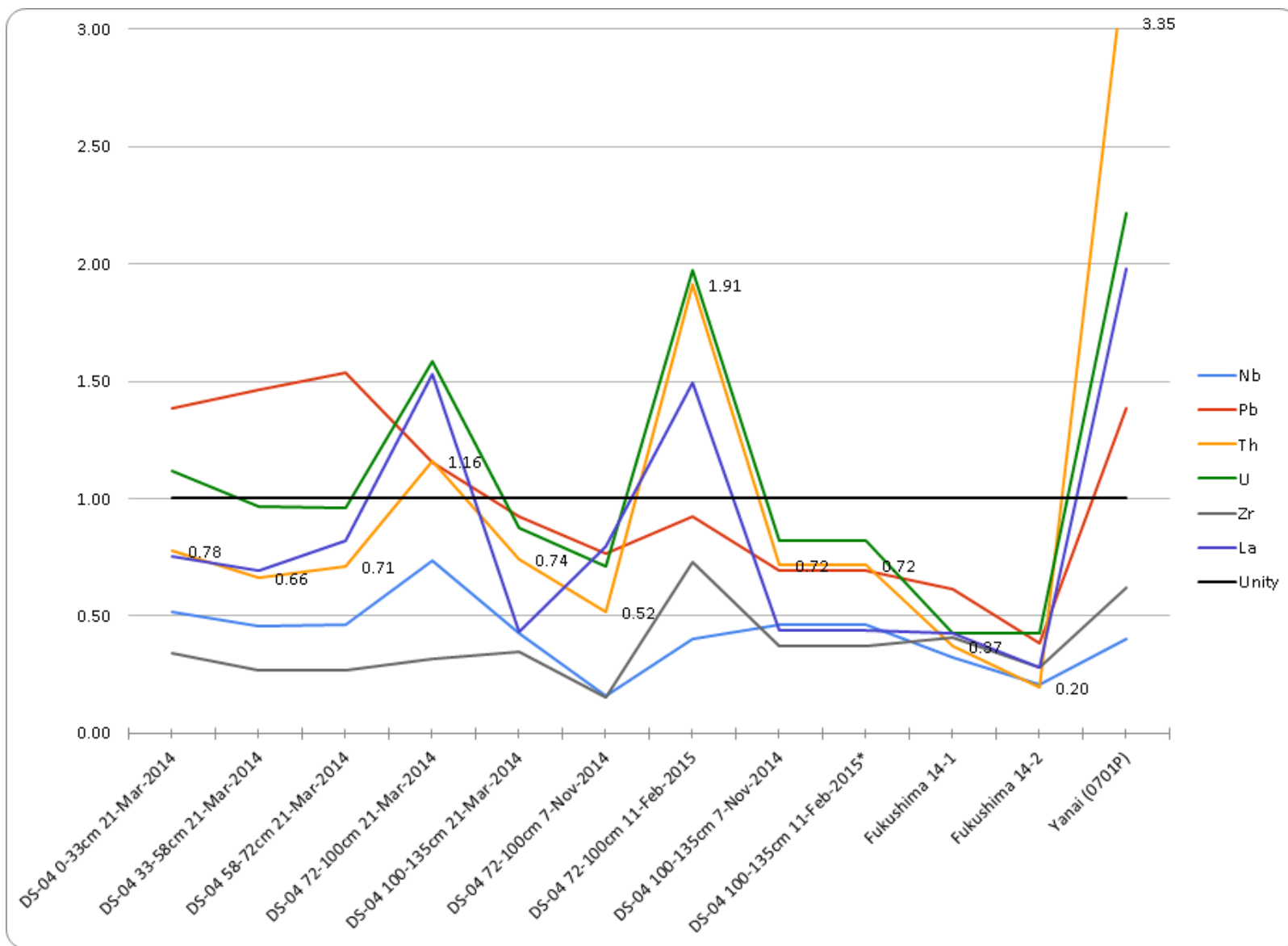


Figure 3.12: Select Rare Earth Metal Enrichments Relative to Average Loess.

3.3 Molar Ratios

The molar ratio values are shown in Table 3-6. These molar ratios are used to characterize the extent of chemical weathering in soils. For example, SA values close to 2 are indicative of moderate levels of chemical weathering or the presence of 1:1 clays. Values between 3.5 and 4.0 indicates the presence of illite and vermiculite. Values above 4.5 are characteristic of weathering where vermiculites and smectites are found as weathering products (Birkeland, 1999). Table 3-6 shows that the samples DS-04 72-100 cm and DS-04 100-135 cm consistently fall within the range that signals the presence of vermiculites.

Table 3-6: Table of Calculated Molar Ratios

Samples	Date	$\frac{\text{SiO}_2}{\text{Al}_2\text{O}_3}$	$\frac{(\text{CaO}+\text{MgO}+\text{Na}_2\text{O}+\text{K}_2\text{O})}{\text{Al}_2\text{O}_3}$	$\frac{\text{SiO}_2}{\text{Fe}_2\text{O}_3}$	$\frac{\text{SiO}_2}{(\text{Al}_2\text{O}_3+\text{Fe}_2\text{O}_3)}$	$\frac{\text{SiO}_2}{(\text{Al}_2\text{O}_3+\text{Fe}_2\text{O}_3+\text{TiO}_2)}$	CIA	A	CN	K
DS-04 0-33cm	21-Mar-2014	4.55	0.71	26.74	3.89	3.77	67.33	67.33	27.94	4.73
DS-04 33-58cm	21-Mar-2014	5.57	0.76	33.56	4.77	4.64	63.04	63.04	31.02	5.94
DS-04 58-72cm	21-Mar-2014	5.16	0.72	31.76	4.44	4.31	64.70	64.70	29.78	5.52
DS-04 72-100cm	21-Mar-2014	3.88	0.49	19.73	3.24	3.12	76.25	76.25	19.62	4.13
DS-04 72-100cm	7-Nov-2014	4.05	0.53	19.05	3.34	3.22	74.75	74.75	21.13	4.12
DS-04 72-100cm	11-Feb-2015	3.88	0.53	19.07	3.22	3.10	74.57	74.57	20.99	4.44
DS-04 100-135cm	21-Mar-2014	4.20	0.57	24.19	3.58	3.46	74.39	74.39	20.71	4.90
DS-04 100-135cm	7-Nov-2014	4.19	0.57	24.53	3.58	3.47	74.68	74.68	20.08	5.24
DS-04 100-135cm	11-Feb-2015	4.12	0.56	24.47	3.52	3.41	74.73	74.73	20.07	5.19
DS-04 100-135cm	25-Feb-2015	4.06	0.55	23.98	3.47	3.36	75.28	75.28	19.67	5.05
Fukushima 14-1	7-Nov-2014	5.63	0.77	19.01	4.34	4.12	70.33	70.33	24.76	4.91
Fukushima 14-2	7-Nov-2014	4.52	0.87	12.31	3.31	3.15	70.79	70.79	26.33	2.89
Yanai (0701P)	11-Feb-2015	6.54	0.73	27.94	5.30	5.06	66.27	66.27	26.94	6.80

Chemical index of alteration (CIA) values serves as a measure of the chemical weathering that has taken place for a particular sample, based on a total major element chemical analysis. Figure 3.13 shows the CIA values of the study samples with reference ranges from Nesbitt and Young (1982). The majority of samples fall within a range consistent with high clay content (shale) and intermediate weathering.

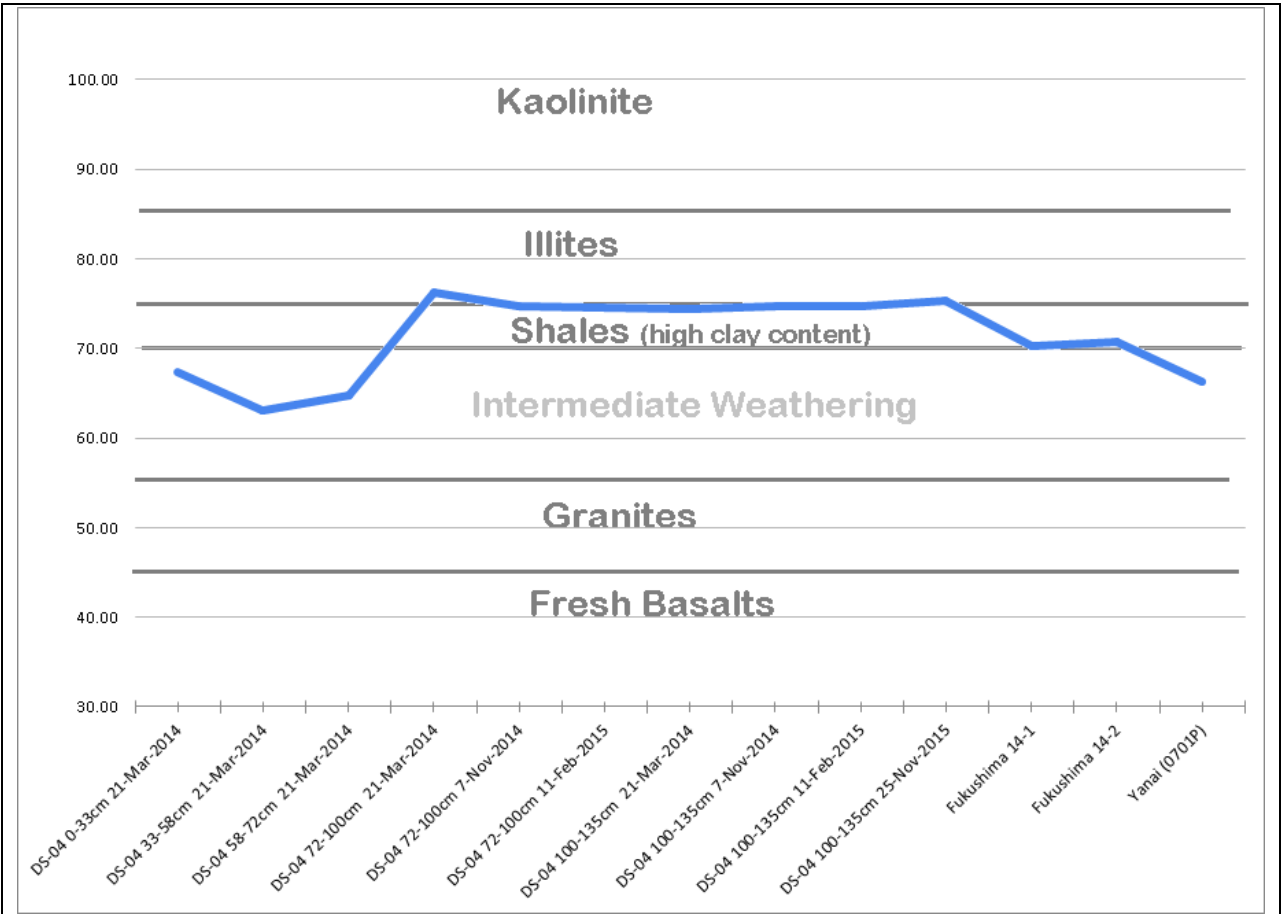


Figure 3.13: Chemical Index of Alteration

4 DISCUSSION

4.1 Soil Chemical Profiles of Japanese Soils

The samples from Mt. Daisen have CIA values and molar ratios that are indicative of weathering that would contain pedogenic vermiculite and illite (as opposed to pedogenic kaolinite or gibbsite). Shaikh (2015) found small amounts of 14Å and 10Å clay minerals in the silt fractions of the same Mt. Daisen samples. The presence of vermiculite and illite are fortuitous relative to the problem of sequestration of accidentally released radioactive Cs. Vermiculite has been shown to adsorb ^{137}Cs up to three orders of magnitude more than other minerals (Sakai et al., 2015). Koarashi et al. (2012) determined that higher ^{137}Cs retention can be explained in part by larger amounts of clay-sized particles. ^{137}Cs retention was found to be negatively correlated with soil organic carbon content (Hasegawa et al., 2015). This negative correlation suggests that strong sorption is inhibited by high levels of organic matter. The enrichment of stable Cs noted in the Mt. Daisen soils relative to upper continental crust shows the potential for the sequestration of ^{137}Cs by these soils at Mt. Daisen in Figure 3.2. The Fukushima samples should likewise be expected to sorb Cs provided 2:1 clays like illite and vermiculite are present in these soils. However, the contents of natural Cs are lower in these soils as seen in Figure 3.2 as well. The explanation of this difference might be resolved from the study of mineralogy of the Fukushima soils and sediments.

It is useful to note too that the Mt. Daisen soils show enriched amounts of Cs relative to other alkali and alkaline earth metals when normalized to upper continental crust. This singular enrichment in Cs relative to the other alkali metals is not expected given data from the Savannah River site near surface soils showing a sympathetic enrichment of alkali and alkaline earth metals

relative to upper continental crust (Zaunbrecher et al., 2015). However, Cs is the most enriched alkali metal in those soils. The factors favoring Cs accumulation in soils relate to mineralogy and clay content in soils.

4.2 Movement of Radiocesium in the Environment

Approximately, 2.5 years after the accident, ^{137}Cs concentrations were found to have increased in the soil layer and decreased in the litter near FDNPP (Hasegawa et al., 2015). Elsewhere in Fukushima Prefecture, radioactive Cs levels further from the reactor are showing decreased radioactivity (mainly Cs, Hasegawa et al., 2015). Furthermore, studies have shown that water soaked litter retains less ^{137}Cs than drier counterparts (Sakai et al., 2015). Leached ^{137}Cs was shown to remain mobile in water only when there were no minerals present, and negligible amounts of ^{137}Cs were found in periodic water sampling (Sakai et al., 2015). The relationship between water content and cesium retention suggests a lower LOI would be correlated with higher retentions of natural cesium, however this was not the case when compared to the Fukushima samples. It is likely the retention of radioactive Cs is a function largely of mineralogy and clay content (e.g. Zaunbrecher et al., 2015).

All of these data attests to the soils ability to sorb the ^{137}Cs from the fallout. Though cesium is often thought of as a mobile ion, the movement of ^{137}Cs in water sources is not an immediate threat considering its sorption by clays. By sorbing ^{137}Cs in soils and the addition of K via fertilizers, the bioavailability of ^{137}Cs to crops is limited (Hasegawa et al., 2015).

Soil retention directly effects the amount of ^{137}Cs available in the environment. Since cesium sorption is thought to be the result of weathered vermiculites, potassium content has an effect on retention. Both the Mt. Daisen samples and the samples found closer to the Fukushima Prefecture show a relative depletion in potassium content. Lower potassium concentrations in

the soil have been shown to increase the uptake of ^{137}Cs by plants (Uematsu et al., 2015).

Uematsu et al., (2015) determined that the transfer of ^{137}Cs from soil to plants is a function of the ^{137}Cs interception potential and the potassium concentration. This means that the transfer of ^{137}Cs sequestered in the soil can be predicted using existing soil maps and application of fertilizers rich in K.

The study by Uematsu, et. al. (2015) showed not only a correlation between soil clay content and plant transfer but also a negative correlation between organic content and plant transfer. This correlation offers an explanation as to why more natural cesium is found in the samples from Mt. Daisen, since the samples from within the Fukushima Prefecture were forested. Normalized amounts of Cs (relative to UCC) is highest from 72-100cm in the Mt. Daisen samples, which falls just above the tephra.

The sequestration of ^{137}Cs in the top layers of the soil by clays is thought to have slowed the re-uptake of ^{137}Cs by plant roots and is illustrated in Figure 4.1 (Shiozawa, 2013; Lasat et al., 1998). Higher levels of organic content within the soil may also serve to block ^{137}Cs interception points (Uematsu et al., 2015). This blockage makes the possibility of phytoremediation in the region unlikely. If no action is taken, it is expected that the magnitude of ^{137}Cs migration in the soil and the uptake of soil ^{137}Cs to overall rice crops will increase gradually over time (Nakanishi and Tanoi, 2013). That being said, it is difficult to determine the contamination to new plants from contaminated soil, since much of the contamination is from direct plant exposure to the fallout (Nakanishi and Tanoi, 2013).

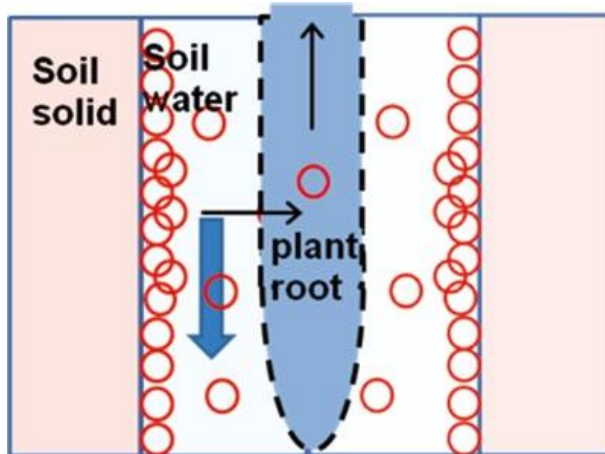


Figure 4.1: Illustration of the Effect of ^{137}Cs Sequestration on Root Uptake (Shiozawa, 2013)

4.3 Potential for Future Studies

The effect of organic matter, clay content and clay mineralogy should be studied to understand further the fixation of ^{137}Cs within the volcanic soils present in Japan. Mt Daisen this site be used as a natural laboratory for further study. This information could be beneficial in the study of remediation for agricultural purposes. Since phytoremediation appears to be less of an option (Shiozawa, 2013), the use of clays to sorb the ^{137}Cs needs to be thoroughly explored.

5 CONCLUSIONS

Chemical analyses on the Mt. Daisen samples shows an enrichment in Fe_2O_3 and natural Cs relative to upper continental crust. These enrichments suggest moderate levels of chemical weathering. Natural cesium was shown to be enriched at all depths within the Mt. Daisen profile compared to upper continental crust, while other alkali metals were shown to be depleted. The Fukushima samples were found to be depleted of natural cesium when compared to UCC. This difference in enrichment of Cs can be explained possibly through further study of the soil mineralogy and clay content. Given the enrichment of natural Cs in the Mt. Daisen soil, radioactive Cs would likely be sorbed by the Mt. Daisen soil.

Molar ratios were calculated for the Mt. Daisen and Fukushima samples in order to identify the existence of clay minerals within the soils. The calculated CIA values fell in a range consistent with intermediate levels of weathering and the presence of pedogenic vermiculites and illites. The identification of this weathering state and projected clay mineral content correlates to higher values of natural cesium in the samples.

This study provides a multi-element chemical analysis of an andisol that is characteristic of soils present within the Fukushima prefecture. This information provides a preliminary understanding of the chemistry between the soils and cesium ions. This knowledge may be used to basis for further study of elemental enrichments and depletions in andisols for elements other than alkali metals. Lastly, this knowledge can be further utilized in the development of remediation techniques.

REFERENCES

- Atomic Energy Society of Japan (2015) *The Fukushima Daiichi Nuclear Accident : final report of the AESJ Investigation Committee*, Tokyo; New York: Springer.
- Bacon, P. and Hobson, C. (2014) *Humanitarian Studies: Human Security and Japan's Triple Disaster: Responding to the 2011 earthquake, tsunami, and Fukushima Nuclear Crisis*, Florence, KY: Routledge.
- Birkeland, P. (1999) *Soils and Geomorphology*, New York: Oxford University Press.
- Blandford, E. and Ahn, J. (2012) 'Examining the Nuclear Accident at Fukushima Daiichi', *Elements*, vol. 8, no. 3, pp. 189-194.
- Bossey, P. (2013) 'Plutonium Emission From the Fukushima Accident', *IRPA Regional Congress on Radiation Protection and Safety, Rio de Janeiro, Brazil*.
- Chino, M., Nakayama, H., Nagai, H., Terada, H., Katata, G. and Yamazawa, H. (2011) 'Preliminary Estimation of Release Amounts of ¹³¹I and ¹³⁷Cs Accidentally Discharged from the Fukushima Daiichi Nuclear Power Plant into the Atmosphere', *Journal of Nuclear Science*, pp. 1129-1134.
- Choi, B.H., Kim, K.O., Min, B.I. and Pelinovsky, E. (2014) 'Transoceanic Propagation of 2011 East Japan Earthquake Tsunami', *Ocean and Polar Research*, vol. 36, no. 3, pp. 225-234.
- Chung, R. (1996) "'The January 17, 1995 Hyogoken-Nanbu (Kobe) Earthquake.'", *NIST Special Publication 901*.
- Endo, S., Kimura, S., Takatsuji, T., Nanasawa, K., Imanaka, T. and Shizuma, K. (2012) 'Measurement of soil contamination by radionuclides due to the Fukushima Dai-ichi Nuclear Power Plant accident and associated estimated cumulative external dose estimation', *Journal of Environmental Radioactivity*, pp. 18-27.

- Harada, M. (1955) 'Studies on the Volcanic Ash Soils in the Environs of Mt. Daisen', *Soil and Plant Food*, vol. 1, no. 1, pp. 81-83.
- Hasegawa, M., Kaneko, S., Ikeda, S., Akama, A., Komatsu, M. and Ito, M. (2015) 'Changes in Radiocesium Concentrations in Epigeic Earthworms in Relation to the Organic Layer 2.5 years after the 2011 Fukushima Dai-ichi Nuclear Power Plant Accident', *Journal of Environmental Radioactivity*, vol. 145, pp. 95-101.
- Kato, H., Onda, Y. and Teramaga, M. (2012) 'Depth distribution of ¹³⁷Cs, ¹³⁴Cs, and ¹³¹I in soil profile after Fukushima Dai-ichi', *Journal of Environmental Radioactivity*, pp. 59-64.
- Kawase, H.(.). (2014) *Studies on the 2011 Off the Pacific Coast of Tohoku Earthquake*, Tokyo, JPN: Springer.
- Koarashi, J., Atarashi-Andoh, M., Matsunaga, T., Sato, T., Nagao, S. and Nagai, H. (2012) 'Factors Affecting Vertical Distribution of Fukushima Accident-derived radiocesium in soil under different land-use conditions', *Science of the Total Environment*, vol. 431, pp. 392-401.
- Kotaki, A., Katoh, S. and Kitani, K. (2011) 'Correlation of Middle Pleistocene crystal-rich tephra layers from Daisen Volcano, southwest Japan, based on chemical composition and refractive index of mafic minerals', *Quaternary International*, vol. 246, pp. 105-117.
- Lasat, M., Fuhrmann, M., Ebbs, S., Cornish, J. and Kochian, L. (1998) 'Phytoremediation of a Radiocesium-Contaminated Soil: Evaluation of Cesium-137 Bioaccumulation in the Shoots of Three Plant Species', *Journal of Environmental Quality*, vol. 27, no. Jan/Feb, pp. 165-173.
- Mathieu, A., Korsakissok, I., Quelo, D., Groell, J., Tombette, M., Didler, D., Quentric, E., Saunler, O., Benolt, J. and Isnard, O. (2012) 'Atmospheric Dispersion and Deposition of

- Radionuclides from the Fukushima Daiichi Nuclear Power Plant Accident', *Elements*, vol. 8, pp. 195-200.
- Matsunaga, T., Koarashi, J., Nagao, S., Atarashi-Andoh, M, Sato, T. and Nagai, H. (2013) 'Comparison of the Vertical Distributions of Fukushima Nuclear Accident Radiocesium in Soil Before and After the First Rainy Season, with Physiochemical and Mineralogical Interpretations', *Science of the Total Environment*, vol. 447, pp. 301-314.
- Nakanishi, T. and Tanoi, K. (2013) *Agricultural Implications of the Fukushima Nuclear Accident*, Tokyo: Springer.
- Nanzyo, M..Y..H.T..Y.I..S.S..a.T.T. (2007) 'Changes in Element Concentrations during Andosol Formation on Tephra in Japan', *European Journal of Soil Science*, vol. 58.2, pp. 465-477.
- Nesbitt, H.W. and Young, G.M. (1982) 'Early Proterozoic Climates and Plate Motions Inferred from Major element chemistry of lutites', *Nature*, vol. 299, no. October, pp. 715-717.
- Ritsema, J., Lay, T. and Kanamori, H. (2012) 'The 2011 Tohoku Earthquake', *Elements*, vol. 8, no. 3, pp. 183-188.
- Sakai, M., Gomi, T., Naito, R., Negishi, J., Sasaki, M., Toda, H., Nunokawa, M. and Murase, K. (2015) 'Radiocesium Leaching From Contaminated Litter in Forest Streams', *Journal of Environmental Radioactivity*, vol. 144, pp. 15-20.
- Shiozawa, S. (2013) 'Vertical Migration of Radiocesium Fallout in Soil in Fukushima', in Nakanishi, T.M. and Tanoi, K. *Agricultural Implications of the Fukushima Nuclear Accident*, Tokyo.
- Soil Survey Staff (2015) *Keys to Soil Taxonomy*, 12th edition, Washington, DC: USDA-Natural Resources Conservation Service.

- Takahashi, T. and Shoji, S. (2002) 'Distribution and Classification of Volcanic Ash Soils', *Global Environmental Research*, pp. 83-97.
- Tsukui, M. (1984) 'Geology of Daisen Volcano', *Journal of the Geological Society of Japan*, vol. 90, no. 9, pp. 643-658.
- Uematsu, S., Smolders, E., Sweeck, L., Wannijin, J., Hees, M.V. and Vandenhove, H. (2015) 'Predicting Radiocesium Sorption Characteristics with Soil Chemical Properties for Japanese Soils', *Science of the Total Environment*, vol. 524, pp. 148-156.
- Wampler, J.M..K.E.J..E.W.C..K.B..a.K.D.I. (2012) 'Long-Term Selective Retention of Natural Cs and Rb by Highly Weathered Coastal Plain Soils', *Environmental Science & Technology*, vol. 46, pp. 3837-3843.
- Yanagi, T. (2011) *Arc volcano of Japan generation of continental crust from the mantle*, Berlin: Springer.
- Yoshida, N. and Takahashi, Y. (2012) 'Land-Surface Contamination by Radionuclides from the Fukushima Daiichi Nuclear Power Plant Accident', *Elements*, vol. 8, pp. 201-206.
- Zhang, F., Zhangdong, J., Li, F., Yu, J., You, C. and Zhou, L. (2013) 'The Dominance of Loess Weathering on Water and Sediment Chemistry within the Daihai Lake Catchment, northeastern Chinese Loess Plateau', *Applied Geochemistry*, vol. 35, pp. 51-63.

Appendix A: Data Tables

Major Element Data

Samples	Date	SiO ₂	Al ₂ O ₃	Fe ₂ O ₃	TiO ₂	P ₂ O ₅	MnO	MgO	CaO	Na ₂ O	K ₂ O	LOI	Total
DS-04 0-33cm	21-Mar-2014	42.15	15.71	4.19	0.453	0.21	0.061	1.39	2.02	1.73	1.02	29.09	98.03
DS-04 33-58cm	21-Mar-2014	42.93	13.09	3.4	0.35	0.16	0.048	0.89	1.86	1.86	1.14	33.04	98.77
DS-04 58-72cm	21-Mar-2014	45.17	14.85	3.78	0.406	0.14	0.058	1.04	1.94	2.01	1.17	27.87	98.42
DS-04 72-100cm	21-Mar-2014	31.55	13.8	4.25	0.516	0.21	0.045	0.99	1.13	0.91	0.69	45.11	99.2
DS-04 72-100cm	7-Nov-2014	31.9	13.37	4.45	0.49	0.21	0.048	1.02	1.21	0.96	0.68	44.66	98.99
DS-04 72-100cm	11-Feb-2015	34.01	14.89	4.74	0.558	0.21	0.048	1.12	1.31	1.1	0.82	42.03	100.8
DS-04 100-135cm	21-Mar-2014	49.23	19.89	5.41	0.618	0.1	0.065	1.79	1.67	1.52	1.21	18.93	100.4
DS-04 100-135cm	7-Nov-2014	49.55	20.05	5.37	0.609	0.11	0.065	1.8	1.58	1.53	1.3	18.24	100.2
DS-04 100-135cm	11-Feb-2015	50.26	20.72	5.46	0.628	0.24	0.063	1.79	1.55	1.67	1.33	17.21	100.9
DS-04 100-135cm	25-Feb-2015	49.8	20.82	5.52	0.638	0.21	0.065	1.79	1.58	1.56	1.29	16.99	100.3
Fukushima 14-1	7-Nov-2014	56.08	16.91	7.84	0.938	0.06	0.103	2.36	2.37	1	1.09	10.45	99.19
Fukushima 14-2	7-Nov-2014	48.11	18.05	10.39	0.983	0.29	0.202	3.23	2.76	1.03	0.68	13.54	99.27
Yanai (0701P)	11-Feb-2015	60.23	15.62	5.73	0.723	0.24	0.085	1.34	2.09	1.55	1.48	9.92	99.01

All data provided by Activation Laboratories, Ltd. Data is displayed as a percentage of the total.

Select Element Data

Samples	Date	Ba	Cs	Rb	Sr	Nb	Pb	Th	U	Zr	La
DS-04 0-33cm	21-Mar-2014	232	5.8	55	281	10.4	18	8.78	2.79	129	26.7
DS-04 33-58cm	21-Mar-2014	261	5.3	62	279	9.1	19	7.49	2.42	100	24.6
DS-04 58-72cm	21-Mar-2014	273	5.3	58	312	9.3	20	8.05	2.4	101	29.1
DS-04 72-100cm	21-Mar-2014	159	9.1	70	147	14.7	15	13.1	3.97	120	54.1
DS-04 72-100cm	7-Nov-2014	157	4.8	34	152	3.2	10	5.84	1.78	57	28.3
DS-04 72-100cm	11-Feb-2015	165	5.1	40	193	8.1	12	21.6	4.94	273	52.9
DS-04 100-135cm	21-Mar-2014	261	5.5	60	257	8.5	12	8.39	2.19	131	15.4
DS-04 100-135cm	7-Nov-2014	272	5.8	60	236	9.3	9	8.13	2.05	140	15.5
DS-04 100-135cm	11-Feb-2015	278	7.5	58	254	9.2	22	270	17.1	376	476
DS-04 100-135cm	25-Feb-2015	268	5.9	57	261	9.3		264	16.3	345	478
Fukushima 14-1	7-Nov-2014	265	3.3	53	108	6.5	8	4.22	1.07	153	15
Fukushima 14-2	7-Nov-2014	296	1.4	34	183	4.2	5	2.21	1.06	106	9.94
Yanai (0701P)	11-Feb-2015	381	3.5	54	141	8.1	18	37.8	5.54	232	70

All data provided by Activation Laboratories, Ltd. Data is shown in parts per million.

Major Element Enrichments Relative to Upper Continental Crust

Samples	Date	SiO ₂	Al ₂ O ₃	Fe ₂ O ₃	TiO ₂	P ₂ O ₅	MnO	MgO	CaO	Na ₂ O	K ₂ O
Upper Cont. Crust	-	65.20	15.60	2.10	0.60	0.20	0.10	2.30	4.70	3.10	3.30
DS-04 0-33cm	21-Mar-2014	0.65	1.01	2.00	0.76	1.05	0.61	0.60	0.43	0.56	0.31
DS-04 33-58cm	21-Mar-2014	0.66	0.84	1.62	0.58	0.80	0.48	0.39	0.40	0.60	0.35
DS-04 58-72cm	21-Mar-2014	0.69	0.95	1.80	0.68	0.70	0.58	0.45	0.41	0.65	0.35
DS-04 72-100cm	21-Mar-2014	0.48	0.88	2.02	0.86	1.05	0.45	0.43	0.24	0.29	0.21
DS-04 72-100cm	7-Nov-2014	0.49	0.86	2.12	0.82	1.05	0.48	0.44	0.26	0.31	0.21
DS-04 72-100cm	11-Feb-2015	0.52	0.95	2.26	0.93	1.05	0.48	0.49	0.28	0.35	0.25
DS-04 100-135cm	21-Mar-2014	0.76	1.28	2.58	1.03	0.50	0.65	0.78	0.36	0.49	0.37
DS-04 100-135cm	7-Nov-2014	0.76	1.29	2.56	1.02	0.55	0.65	0.78	0.34	0.49	0.39
DS-04 100-135cm	11-Feb-2015	0.77	1.33	2.60	1.05	1.20	0.63	0.78	0.33	0.54	0.40
DS-04 100-135cm	25-Feb-2015	0.76	1.33	2.63	1.06	1.05	0.65	0.78	0.34	0.50	0.39
Fukushima 14-1	7-Nov-2014	0.86	1.08	3.73	1.56	0.30	1.03	1.03	0.50	0.32	0.33
Fukushima 14-2	7-Nov-2014	0.74	1.16	4.95	1.64	1.45	2.02	1.40	0.59	0.33	0.21
Yanai (0701P)	11-Feb-2015	0.92	1.00	2.73	1.21	1.20	0.85	0.58	0.44	0.50	0.45

Samples normalized to upper continental crust based on values from Yanagi (2011).

Select Element Enrichments Relative to Upper Continental Crust

Samples	Date	Ba	Cs	Rb	Sr	Nb	Pb	Th	U	Zr	La
Upper Continental Crust	-	550.00	3.70	112.00	350.00	25.00	20.00	10.70	2.80	190.00	30.00
DS-04 0-33cm	21-Mar-2014	0.42	1.57	0.49	0.80	0.42	0.90	0.82	1.00	0.68	0.89
DS-04 33-58cm	21-Mar-2014	0.47	1.43	0.55	0.80	0.36	0.95	0.70	0.86	0.53	0.82
DS-04 58-72cm	21-Mar-2014	0.50	1.43	0.52	0.89	0.37	1.00	0.75	0.86	0.53	0.97
DS-04 72-100cm	21-Mar-2014	0.29	2.46	0.63	0.42	0.59	0.75	1.22	1.42	0.63	1.80
DS-04 72-100cm	7-Nov-2014	0.29	1.30	0.30	0.43	0.13	0.50	0.55	0.64	0.30	0.94
DS-04 72-100cm	11-Feb-2015	0.30	1.38	0.36	0.55	0.32	0.60	2.02	1.76	1.44	1.76
DS-04 100-135cm	21-Mar-2014	0.47	1.49	0.54	0.73	0.34	0.60	0.78	0.78	0.69	0.51
DS-04 100-135cm	7-Nov-2014	0.49	1.57	0.54	0.67	0.37	0.45	0.76	0.73	0.74	0.52
DS-04 100-135cm	11-Feb-2015	0.51	2.03	0.52	0.73	0.37	1.10	25.23	6.11	1.98	15.87
DS-04 100-135cm	25-Feb-2015	0.49	1.59	0.51	0.75	0.37	0.00	24.67	5.82	1.82	15.93
Fukushima 14-1	7-Nov-2014	0.48	0.89	0.47	0.31	0.26	0.40	0.39	0.38	0.81	0.50
Fukushima 14-2	7-Nov-2014	0.54	0.38	0.30	0.52	0.17	0.25	0.21	0.38	0.56	0.33
Yanai (0701P)	11-Feb-2015	0.69	0.95	0.48	0.40	0.32	0.90	3.53	1.98	1.22	2.33

Samples normalized to upper continental crust per Yanagi (2011).

Major Element Enrichments Relative to Average Japanese Andisol

Samples	Date	SiO ₂	Al ₂ O ₃	Fe ₂ O ₃	TiO ₂	P ₂ O ₅	MnO	MgO	CaO	Na ₂ O	K ₂ O
Ave. Japanese Andisol	-	43.00	22.00	10.00	1.10	0.20	0.18	2.10	2.10	1.10	0.88
DS-04 0-33cm	21-Mar-2014	0.98	0.71	0.42	0.41	1.05	0.34	0.66	0.96	1.57	1.16
DS-04 33-58cm	21-Mar-2014	1.00	0.60	0.34	0.32	0.80	0.27	0.42	0.89	1.69	1.30
DS-04 58-72cm	21-Mar-2014	1.05	0.68	0.38	0.37	0.70	0.32	0.50	0.92	1.83	1.33
DS-04 72-100cm	21-Mar-2014	0.73	0.63	0.43	0.47	1.05	0.25	0.47	0.54	0.83	0.78
DS-04 72-100cm	7-Nov-2014	0.74	0.61	0.45	0.45	1.05	0.27	0.49	0.58	0.87	0.77
DS-04 72-100cm	11-Feb-2015	0.79	0.68	0.47	0.51	1.05	0.27	0.53	0.62	1.00	0.93
DS-04 100-135cm	21-Mar-2014	1.14	0.90	0.54	0.56	0.50	0.36	0.85	0.80	1.38	1.38
DS-04 100-135cm	7-Nov-2014	1.15	0.91	0.54	0.55	0.55	0.36	0.86	0.75	1.39	1.48
DS-04 100-135cm	11-Feb-2015	1.17	0.94	0.55	0.57	1.20	0.35	0.85	0.74	1.52	1.51
DS-04 100-135cm	25-Feb-2015	1.16	0.95	0.55	0.58	1.05	0.36	0.85	0.75	1.42	1.47
Fukushima 14-1	7-Nov-2014	1.30	0.77	0.78	0.85	0.30	0.57	1.12	1.13	0.91	1.24
Fukushima 14-2	7-Nov-2014	1.12	0.82	1.04	0.89	1.45	1.12	1.54	1.31	0.94	0.77
Yanai (0701P)	11-Feb-2015	1.40	0.71	0.57	0.66	1.20	0.47	0.64	1.00	1.41	1.68

Samples normalized to average Japanese Andisols per Takeda et al. (2004).

Select Element Enrichments Relative to Average Japanese Andisol

Samples	Date	Ba	Cs	Rb	Sr	Nb	Pb	Th	U	Zr	La
Average Japanese Andisol	-	290.00	4.00	44.00	130.00	7.30	23.00	6.40	1.50	110.00	20.00
DS-04 0-33cm	21-Mar-2014	0.80	1.45	1.25	2.16	1.42	0.78	1.37	1.86	1.17	1.34
DS-04 33-58cm	21-Mar-2014	0.90	1.33	1.41	2.15	1.25	0.83	1.17	1.61	0.91	1.23
DS-04 58-72cm	21-Mar-2014	0.94	1.33	1.32	2.40	1.27	0.87	1.26	1.60	0.92	1.46
DS-04 72-100cm	21-Mar-2014	0.55	2.28	1.59	1.13	2.01	0.65	2.05	2.65	1.09	2.71
DS-04 72-100cm	7-Nov-2014	0.54	1.20	0.77	1.17	0.44	0.43	0.91	1.19	0.52	1.42
DS-04 72-100cm	11-Feb-2015	0.57	1.28	0.91	1.48	1.11	0.52	3.38	3.29	2.48	2.65
DS-04 100-135cm	21-Mar-2014	0.90	1.38	1.36	1.98	1.16	0.52	1.31	1.46	1.19	0.77
DS-04 100-135cm	7-Nov-2014	0.94	1.45	1.36	1.82	1.27	0.39	1.27	1.37	1.27	0.78
DS-04 100-135cm	11-Feb-2015	0.96	1.88	1.32	1.95	1.26	0.96	42.19	11.40	3.42	23.80
DS-04 100-135cm	25-Feb-2015	0.92	1.48	1.30	2.01	1.27	0.00	41.25	10.87	3.14	23.90
Fukushima 14-1	7-Nov-2014	0.91	0.83	1.20	0.83	0.89	0.35	0.66	0.71	1.39	0.75
Fukushima 14-2	7-Nov-2014	1.02	0.35	0.77	1.41	0.58	0.22	0.35	0.71	0.96	0.50
Yanai (0701P)	11-Feb-2015	1.31	0.88	1.23	1.08	1.11	0.78	5.91	3.69	2.11	3.50

Samples normalized to average Japanese Andisols per Takeda et al. (2004).

Select Element Enrichments Relative to Loess

Samples	Date	Ba	Cs	Rb	Sr	Nb	Pb	Th	U	Zr	La
Average Loess	-	625.00	4.00	85.00	192.00	20.00	13.00	11.30	2.50	375.00	35.40
DS-04 0-33cm	21-Mar-2014	58.00	1.45	0.65	1.46	0.52	1.38	0.78	1.12	0.34	0.75
DS-04 33-58cm	21-Mar-2014	0.42	1.33	0.73	1.45	0.46	1.46	0.66	0.97	0.27	0.69
DS-04 58-72cm	21-Mar-2014	0.44	1.33	0.68	1.63	0.47	1.54	0.71	0.96	0.27	0.82
DS-04 72-100cm	21-Mar-2014	0.25	2.28	0.82	0.77	0.74	1.15	1.16	1.59	0.32	1.53
DS-04 72-100cm	7-Nov-2014	0.25	1.20	0.40	0.79	0.16	0.77	0.52	0.71	0.15	0.80
DS-04 72-100cm	11-Feb-2015	0.26	1.28	0.47	1.01	0.41	0.92	1.91	1.98	0.73	1.49
DS-04 100-135cm	21-Mar-2014	0.42	1.38	0.71	1.34	0.43	0.92	0.74	0.88	0.35	0.44
DS-04 100-135cm	7-Nov-2014	0.44	1.45	0.71	1.23	0.47	0.69	0.72	0.82	0.37	0.44
DS-04 100-135cm	11-Feb-2015	0.44	1.88	0.68	1.32	0.46	1.69	23.89	6.84	1.00	13.45
DS-04 100-135cm	25-Feb-2015	0.43	1.48	0.67	1.36	0.47	0.00	23.36	6.52	0.92	13.50
Fukushima 14-1	7-Nov-2014	0.42	0.83	0.62	0.56	0.33	0.62	0.37	0.43	0.41	0.42
Fukushima 14-2	7-Nov-2014	0.47	0.35	0.40	0.95	0.21	0.38	0.20	0.42	0.28	0.28
Yanai (0701P)	11-Feb-2015	0.61	0.88	0.64	0.73	0.41	1.38	3.35	2.22	0.62	1.98

Samples normalized to loess as Taylor & McLennan (1985)

Major Element Enrichments Relative to Loess

Samples	Date	SiO ₂	Al ₂ O ₃	Fe ₂ O ₃	TiO ₂	P ₂ O ₅	MnO	MgO	CaO	Na ₂ O	K ₂ O
Average Loess	-	66.58	11.92	4.82	0.67	0.14	0.09	1.96	5.61	1.25	2.61
DS-04 0-33cm	21-Mar-2014	0.63	1.32	0.87	0.68	1.50	0.68	0.71	0.36	1.38	0.39
DS-04 33-58cm	21-Mar-2014	0.64	1.10	0.71	0.52	1.14	0.53	0.45	0.33	1.49	0.44
DS-04 58-72cm	21-Mar-2014	0.68	1.25	0.78	0.61	1.00	0.64	0.53	0.35	1.61	0.45
DS-04 72-100cm	21-Mar-2014	0.47	1.16	0.88	0.77	1.50	0.50	0.51	0.20	0.73	0.26
DS-04 72-100cm	7-Nov-2014	0.48	1.12	0.92	0.73	1.50	0.53	0.52	0.22	0.77	0.26
DS-04 72-100cm	11-Feb-2015	0.51	1.25	0.98	0.83	1.50	0.53	0.57	0.23	0.88	0.31
DS-04 100-135cm	21-Mar-2014	0.74	1.67	1.12	0.92	0.71	0.72	0.91	0.30	1.22	0.46
DS-04 100-135cm	7-Nov-2014	0.74	1.68	1.11	0.91	0.79	0.72	0.92	0.28	1.22	0.50
DS-04 100-135cm	11-Feb-2015	0.75	1.74	1.13	0.94	1.71	0.70	0.91	0.28	1.34	0.51
DS-04 100-135cm	25-Feb-2015	0.75	1.75	1.15	0.95	1.50	0.72	0.91	0.28	1.25	0.49
Fukushima 14-1	7-Nov-2014	0.84	1.42	1.63	1.40	0.43	1.14	1.20	0.42	0.80	0.42
Fukushima 14-2	7-Nov-2014	0.72	1.51	2.16	1.47	2.07	2.24	1.65	0.49	0.82	0.26
Yanai (0701P)	11-Feb-2015	0.90	1.31	1.19	1.08	1.71	0.94	0.68	0.37	1.24	0.57

Samples normalized to loess as Taylor & McLennan (1985)

Major Element Molar Calculations

Samples	Date	SiO ₂	Al ₂ O ₃	Fe ₂ O ₃	TiO ₂	P ₂ O ₅	MnO	MgO	CaO	Na ₂ O	K ₂ O
Oxide Molar Masses		60.08	101.96	159.69	79.87	283.89	70.94	40.3	56.08	61.97	94.2
DS-04 0-33cm	21-Mar-2014	0.702	0.154	0.026	0.006	0.001	0.001	0.034	0.036	0.028	0.011
DS-04 33-58cm	21-Mar-2014	0.715	0.128	0.021	0.004	0.001	0.001	0.022	0.033	0.030	0.012
DS-04 58-72cm	21-Mar-2014	0.752	0.146	0.024	0.005	0.000	0.001	0.026	0.035	0.032	0.012
DS-04 72-100cm	21-Mar-2014	0.525	0.135	0.027	0.006	0.001	0.001	0.025	0.020	0.015	0.007
DS-04 72-100cm	7-Nov-2014	0.531	0.131	0.028	0.006	0.001	0.001	0.025	0.022	0.015	0.007
DS-04 72-100cm	11-Feb-2015	0.566	0.146	0.030	0.007	0.001	0.001	0.028	0.023	0.018	0.009
DS-04 100-135cm	21-Mar-2014	0.819	0.195	0.034	0.008	0.000	0.001	0.044	0.030	0.025	0.013
DS-04 100-135cm	7-Nov-2014	0.825	0.197	0.034	0.008	0.000	0.001	0.045	0.028	0.025	0.014
DS-04 100-135cm	11-Feb-2015	0.837	0.203	0.034	0.008	0.001	0.001	0.044	0.028	0.027	0.014
DS-04 100-135cm	25-Feb-2015	0.829	0.204	0.035	0.008	0.001	0.001	0.044	0.028	0.025	0.014
Fukushima 14-1	7-Nov-2014	0.933	0.166	0.049	0.012	0.000	0.001	0.059	0.042	0.016	0.012
Fukushima 14-2	7-Nov-2014	0.801	0.177	0.065	0.012	0.001	0.003	0.080	0.049	0.017	0.007
Yanai (0701P)	11-Feb-2015	1.002	0.153	0.036	0.009	0.001	0.001	0.033	0.037	0.025	0.016

Molar calculations based on 100g samples / molar weight of the element

Major Element Analysis Molar Ratios

Samples	Date	$\frac{\text{SiO}_2}{\text{Al}_2\text{O}_3}$	$\frac{(\text{CaO}+\text{MgO}+\text{Na}_2\text{O}+\text{K}_2\text{O})}{\text{Al}_2\text{O}_3}$	$\frac{\text{SiO}_2}{\text{Fe}_2\text{O}_3}$	$\frac{\text{SiO}_2}{(\text{Al}_2\text{O}_3+\text{Fe}_2\text{O}_3)}$	$\frac{\text{SiO}_2}{(\text{Al}_2\text{O}_3+\text{Fe}_2\text{O}_3+\text{TiO}_2)}$	CIA	A	CN	K
DS-04 0-33cm	21-Mar-2014	4.55	0.71	26.74	3.89	3.77	67.33	67.33	27.94	4.73
DS-04 33-58cm	21-Mar-2014	5.57	0.76	33.56	4.77	4.64	63.04	63.04	31.02	5.94
DS-04 58-72cm	21-Mar-2014	5.16	0.72	31.76	4.44	4.31	64.70	64.70	29.78	5.52
DS-04 72-100cm	21-Mar-2014	3.88	0.49	19.73	3.24	3.12	76.25	76.25	19.62	4.13
DS-04 72-100cm	7-Nov-2014	4.05	0.53	19.05	3.34	3.22	74.75	74.75	21.13	4.12
DS-04 72-100cm	11-Feb-2015	3.88	0.53	19.07	3.22	3.10	74.57	74.57	20.99	4.44
DS-04 100-135cm	21-Mar-2014	4.20	0.57	24.19	3.58	3.46	74.39	74.39	20.71	4.90
DS-04 100-135cm	7-Nov-2014	4.19	0.57	24.53	3.58	3.47	74.68	74.68	20.08	5.24
DS-04 100-135cm	11-Feb-2015	4.12	0.56	24.47	3.52	3.41	74.73	74.73	20.07	5.19
DS-04 100-135cm	25-Feb-2015	4.06	0.55	23.98	3.47	3.36	75.28	75.28	19.67	5.05
Fukushima 14-1	7-Nov-2014	5.63	0.77	19.01	4.34	4.12	70.33	70.33	24.76	4.91
Fukushima 14-2	7-Nov-2014	4.52	0.87	12.31	3.31	3.15	70.79	70.79	26.33	2.89
Yanai (0701P)	11-Feb-2015	6.54	0.73	27.94	5.30	5.06	66.27	66.27	26.94	6.80

Calculations based on molar calculations from previous table.